
SEISMO: Increasing Sample Efficiency in Molecular Optimization with a Trajectory-Aware LLM Agent

Fabian P. Krüger^{*123} Andrea Hunklinger^{*34} Adrian Wolny³ Tim J. Adler³ Igor Tetko²
Santiago David Villalba³

Abstract

Optimizing the structure of molecules to achieve desired properties is a central bottleneck across the chemical sciences, particularly in the pharmaceutical industry where it underlies the discovery of new drugs. Since molecular property evaluation often relies on costly and rate-limited oracles, such as experimental assays, molecular optimization must be highly sample-efficient. To address this, we introduce SEISMO, an LLM agent that performs strictly online, inference-time molecular optimization, updating after every oracle call without the need for population-based or batched learning. SEISMO conditions each proposal on the full optimization trajectory, combining natural-language task descriptions with scalar scores and, when available, structured explanatory feedback. Across the Practical Molecular Optimization benchmark of 23 tasks, SEISMO achieves a 2–3 times higher area under the optimisation curve than prior methods, often reaching near-maximal task scores within 50 oracle calls. Our additional medicinal-chemistry tasks show that providing explanatory feedback further improves efficiency, demonstrating that leveraging domain knowledge and structured information is key to sample-efficient molecular optimization.

1. Introduction

Generating molecules with desired properties is a central goal in chemistry. A prominent example is the pharmaceutical industry, which requires the discovery of novel molecules in order to bring new drugs to the market. Such molecules must satisfy multiple objectives, including potency, selectivity, and a range of pharmacokinetic and physicochemical properties (Lipinski et al., 2012), which can conflict and therefore require explicit trade-offs. At the same time, the searchable chemical space is enormous, often estimated at around 10^{60} plausible small drug-like molecules (Bohacek et al., 1996).

Because this chemical space is far too large to be explored exhaustively, practical molecular design is instead carried out as an iterative optimization process in which candidate molecules are proposed, evaluated, and refined over successive steps (Ghiandoni et al., 2024). For the evaluations, experimental assays provide the most reliable assessment of molecular properties, but their high cost and limited throughput make them impractical for use at every iteration. As a result, molecular optimization pipelines rely on computational methods that approximate experimental outcomes (Ghiandoni et al., 2024). In practice, these methods span a spectrum of cost and fidelity: lower-cost approximations often provide weaker correlations with experimental measurements, while more accurate approaches, such as physics-based simulations and protein–ligand co-folding methods, are computationally expensive and rate-limited (Meli et al., 2022; Passaro et al., 2025; Abramson et al., 2024). Reducing the number of required evaluations therefore has direct practical value: sample-efficient optimization methods enable the use of higher-quality evaluations, which in turn leads to molecules that are more likely to perform well in practice.

To systematically assess sample efficiency in molecular optimization, the Practical Molecular Optimization (PMO) benchmark was introduced, consisting of a diverse set of molecular design tasks (Gao et al., 2022). Results reported for PMO show that current reinforcement learning and genetic algorithm methods can achieve strong final performance, but they typically still require thousands of evalua-

^{*}Equal contribution ¹Technical University of Munich, Germany; TUM School of Computation, Information and Technology, Department of Mathematics ²Helmholtz Munich – German Research Center for Environmental Health (GmbH), Institute of Structural Biology, Molecular Targets and Therapeutics Center, 85764 Neuherberg, Germany ³Bayer AG; Machine Learning Research ⁴Universitat de Barcelona, Facultat de Farmàcia i Ciències de l’Alimentació, Avda. Diagonal 643, Barcelona 08028, Spain. Correspondence to: Fabian Krüger <fabian.krueger@tum.de>, Andrea Hunklinger <andi.hunklinger@bayer.com>, Santiago David Villalba <santiago.villalba@bayer.com>.

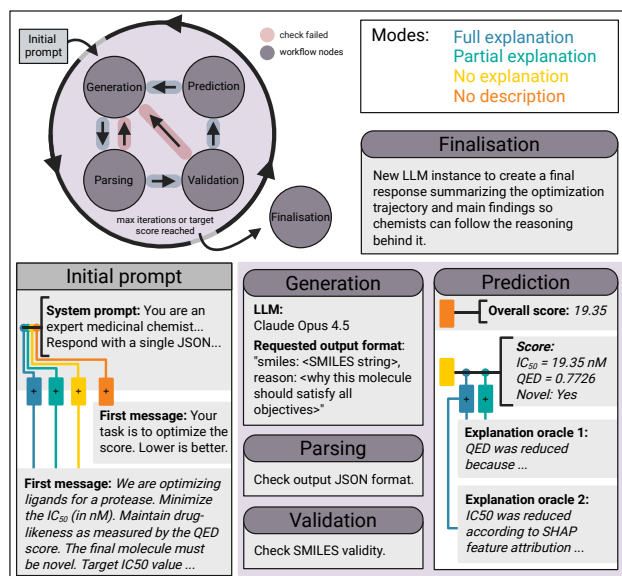


Figure 1. Overview of the iterative optimisation cycle of SEISMO. The initial message and prediction feedback are modular and vary between tasks. Colors indicate different levels of information available in different agent modes, corresponding to the evaluation settings used to analyse performance. Italicized text shows an example. The full system prompt and an example conversation are provided in Appendix E.

tions to do so. As a result, their practical applicability depends on the availability of large evaluation budgets, which may be prohibitive when evaluations are expensive or rate-limited.

We hypothesize that sample efficiency in molecular optimization can be improved by more effectively leveraging available chemical and biological prior knowledge, rather than framing optimization as a purely black-box search driven only by scalar objective values. Motivated by this, we introduce a goal-directed, highly efficient large language model (LLM) agent that we call SEISMO (Sample-Efficient Inference-Stage Molecular-Optimization agent). SEISMO uses the LLM itself as the optimizer and performs strictly online, inference-time molecular optimization by conditioning each proposal on the full optimization trajectory, including prior knowledge and oracle feedback.

2. Related work

Molecular optimisation in drug discovery is commonly framed as black-box search over chemical space, with approaches ranging from objective-guided generative models to population-based and surrogate-assisted search. REINVENT exemplifies the first class, optimising a molecule generator via policy-gradient reinforcement learning using batch-level scalar rewards (Olivecrona et al., 2017). Graph-GA is a standard baseline for the second class, evolving

molecules through graph-based crossover and mutation operators (Jensen, 2019). Gaussian process Bayesian optimisation (GP BO) is another widely used approach, fitting a surrogate over molecular fingerprints and selecting candidates via acquisition functions (Tripp et al., 2021).

Follow-up work has explored improving the sample efficiency of REINVENT-style methods, with Augmented Memory (Guo & Schwaller, 2024) and Beam Enumeration (Guo & Schwaller, 2023) reusing and filtering previously evaluated molecules through experience replay, SMILES augmentation, or substructure-based conditioning. Despite these improvements, optimisation proceeds in fixed batches, imposing a minimum number of oracle calls between policy updates.

Recent methods incorporate LLMs into population-based molecular search. MolLEO extends Graph-GA by using an LLM to perform crossover and mutation operations based on parent molecules (Wang et al., 2024). Unlike MolLEO, LICO uses an evolutionary algorithm to generate candidate molecules via standard crossover and mutation, and employs an LLM as a surrogate model to predict a mean and standard deviation for these candidates, selecting evaluations using an acquisition function (Nguyen & Grover, 2024).

In contrast to prior molecular optimisation methods, SEISMO treats optimisation itself as an inference-time, sequential decision process executed entirely within the LLM’s context, where each oracle call immediately updates the state on which the next proposal is conditioned. Rather than learning a policy, surrogate, or population dynamics, SEISMO relies on trajectory-level reasoning over past molecules, scores, and feedback, making the optimisation history the central learning signal.

LLM-based agents in chemistry have recently emerged to support scientific workflows. ChemAgent (Tang et al., 2025) and CACTUS (McNaughton et al., 2024) target free-form chemistry question answering by augmenting LLM reasoning with external tools such as literature search and standard cheminformatics libraries, while DrugAgent (Inoue et al., 2025) focuses on drug–target interaction prediction.

Other systems extend this agentic framing to broader end-to-end assistance in medicinal chemistry. ChemCrow (Bran et al., 2024) and Frogent (Pan et al., 2025) integrate tool use for information retrieval, synthesis planning, and workflow execution, with ChemCrow additionally enabling autonomous laboratory execution. MADD (Solovev et al., 2025) similarly emphasizes early-stage hit identification by coupling LLM agents to specialised drug-design tools. Across these approaches, the LLM primarily acts as a controller that orchestrates external tools, while optimisation itself is delegated to learned models, heuristics, or downstream pipelines.

In contrast to prior agentic work, SEISMO focuses narrowly on goal-directed molecular optimisation under a strict oracle budget. Rather than acting as a controller over external tools, the LLM itself serves as the optimiser, directly coupling generation with iterative oracle feedback. Additionally, SEISMO augments scalar oracle scores with explanation-based signals from post-hoc explainability methods (XAI), which, to our knowledge, have not been used as control signals in molecular optimisation.

3. Problem formulation

The molecular optimisation problem is the task of finding a molecule $m \in M$ that maximises the score of an evaluation function $F : M \rightarrow \mathbb{R}$. Formally,

$$m^* \in \operatorname{argmax}_{m \in M} F(m).$$

Although F is often treated as a black-box objective in molecular optimisation, in practice this abstraction discards substantial additional information that is typically available in real world settings.

First, $F(m)$ is usually an aggregation of multiple property scores,

$$F(m) = \sum_{k=1}^K w_k f_k(m),$$

where the individual components $f_k(m)$ and their weights w_k are available information in addition to the aggregated score.

Second, for tasks of direct scientific or industrial relevance — such as optimising drug-like properties or binding affinity to a target protein — there usually exists substantial prior knowledge about the different properties f_k , accumulated through decades of chemical and biological research. This knowledge includes, for example, well-characterized functional-group effects, structural alerts and other medicinal-chemistry heuristics, synthetic feasibility considerations, and established structure–property relationships. Such domain knowledge can inform and constrain the search over candidate molecules even when F itself is only accessible via queries.

Third, since many such properties are expensive to evaluate experimentally, each $f_k(m)$ is typically obtained via computational approximations, for example via learned surrogate predictors. This allows for post-hoc explainability methods (e.g. Shapley Additive Explanations (SHAP) (Lundberg & Lee, 2017)) that provide further insights into why a candidate molecule receives a particular score. We model this via an explainer G that returns a structured explanation \mathcal{E} and a natural-language verbalizer that converts the structured explanation as a textual rationale:

$$G : \mathcal{F} \times M \rightarrow \mathcal{E} \quad \text{verbalize} : \mathcal{E} \rightarrow \Sigma_{\text{NL}}^*,$$

where \mathcal{F} denotes the space of evaluation functions, i.e., $F \in \mathcal{F}$.

Our goal is to increase sample efficiency in molecular optimisation by leveraging these additional sources of information.

4. Approach

A natural way to incorporate the aforementioned priors and side-information is through LLMs. As LLMs are trained on large, heterogeneous text corpora that include substantial scientific and technical content, they can serve as a practical proxy for the kind of accumulated domain knowledge described above. While such knowledge is not guaranteed to be perfectly accurate or complete, it provides an inductive bias that can guide the search toward plausible, high-scoring regions of chemical space.

Crucially, LLMs operate on natural language, which makes it straightforward to provide rich, structured feedback beyond a scalar objective. In particular, we can supply the agent with the task description, the sub-score decomposition $f_k(m)_{k=1}^K$, and property-level explanations produced by G . This turns each molecule evaluation into an informative observation rather than a single number.

Motivated by this, we construct a goal-directed LLM agent that performs inference-time optimisation via iterative interaction with an evaluation environment.

Let $d \in \Sigma_{\text{NL}}^*$ denote the initial natural-language problem description (task context and any available prior constraints). At iteration $t \in \{1, \dots, T\}$, the agent proposes a molecule based on the context and the history of previous trials:

$$m_t \sim \pi_{\text{LLM}}(\cdot \mid d, H_{t-1}),$$

where H_{t-1} is the history (see below) and π_{LLM} is the proposal policy obtained by sampling from an LLM with fixed weights and mapping the generated strings to molecules (via SMILES parsing), thereby inducing a conditional distribution over M given (d, H_{t-1}) . The environment then returns not only the aggregate score but also its decomposition and explanations,

$$y_t = \left(F(m_t), (f_k(m_t))_{k=1}^K, (r_{t,k})_{k=1}^K \right),$$

where $r_{t,k} \in \Sigma_{\text{NL}}^*$ is a textual explanation for the component score $f_k(m_t)$. The history is updated by appending the new trial and feedback,

$$H_t = H_{t-1} \cup \{(m_t, y_t)\}.$$

The update from H_{t-1} to H_t after every evaluation induces an online optimisation process with update frequency one per sample, rather than one per batch. This removes the

lower bound on sample efficiency imposed by population-based or batched acquisition schemes used in many existing methods. After a budget of T evaluations, the agent outputs the best molecule encountered,

$$\hat{m}_T \in \operatorname{argmax}_{t \in \{1, \dots, T\}} F(m_t).$$

In this setup, optimisation happens at inference time through the evolving context (d, H_t) : the agent repeatedly conditions on prior knowledge (encoded in d and the LLM) and on increasingly informative feedback (scores, breakdowns, and explanations) to guide subsequent proposals toward higher-scoring molecules with improved sample efficiency.

5. Experiments

We implement SEISMO as a stateful LLM workflow that realizes the trajectory-conditioned, inference-time optimization procedure described above. Figure 1 provides an overview of the workflow. The concrete workflow graph structure, validation logic, prompting, and implementation are described in detail in Appendix A. An ablation study of the LLM backbone is provided in Appendix B. An example output trajectory is shown in Appendix E.4.

Overall, we perform three experiments. First, we evaluate SEISMO on the established PMO benchmark. Then we perform an experiment to more directly mirror common medicinal-chemistry optimization loops (drug-discovery workflow proxies). Unlike PMO, these tasks use oracles under our control, allowing us to not only assess SEISMO’s general drug-discovery performance, but to investigate the influence of additional explanatory feedback beyond the scalar score on performance metrics. Lastly, we qualitatively evaluate SEISMO in co-folding-based optimization regimes where simple surrogate oracles are inadequate. To this end, we use a more expressive but computationally expensive protein–ligand structure prediction oracle based on the Boltz-2 model (Passaro et al., 2025) to evaluate SEISMO on a target with no known binders and limited task-specific prior knowledge. The following paragraphs describe each experiment and their results in more detail.

5.1. PMO benchmark

Setup: We evaluate SEISMO on the PMO benchmark of 23 molecule optimization tasks (Gao et al., 2022). For a fair comparison with prior work, we use the original PMO oracles and provide the agent only with the scalar oracle score at each iteration, without additional explanation. We compare SEISMO to established molecular optimization baselines, including REINVENT, Graph-GA, and Gaussian-process Bayesian optimization (Olivecrona et al., 2017; Jensen, 2019; Tripp et al., 2021). Then, to provide a broader comparison against more recent approaches, we compare

against the results reported by Nguyen and Grover (Nguyen & Grover, 2024), which include a wide range of optimization models such as MolLeo and LICO.

We consider two SEISMO variants: In the *task described* variant, the optimization objective is stated in the initial prompt using descriptions (cf. Appendix E.2) comparable to those used in other work (Wang et al., 2024). In the *no description* variant, the initial prompt omits any description of the objective and the agent treats the oracle as fully black-box. For each task, we run both variants for three independent repetitions with a budget of 50 oracle calls.

Following PMO, we evaluate sample efficiency using the area under the optimization curve (AUC). The optimization curve tracks the best oracle score achieved up to a given oracle call and is defined as

$$s_t = \max_{i \leq t} F(m_i),$$

where $F(m_t) \in [0, 1]$ is the oracle score of the molecule evaluated at oracle call t . AUC is defined as the area under s_t , normalized by the oracle budget, such that AUC values lie in $[0, 1]$. Higher AUC values correspond to faster discovery of high-scoring molecules.

We report top-1 AUC over 50 oracle calls and over 10,000 oracle calls. We also report the best score achieved after 50 oracle calls, defined as $s_{50} = \max_{i \leq 50} F(m_i)$. For comparison to recent work (Nguyen & Grover, 2024), we additionally report top-10 AUC over 1,000 oracle calls, where the optimization curve tracks the average score of the ten best molecules found so far at each oracle call.

For metrics evaluated beyond 50 oracle calls, SEISMO is only allowed to propose molecules during the first 50 calls. For $t > 50$ we hold s_t fixed at its value after 50 calls, while other methods continue optimizing over the full budget. This is due to LLM API cost given the number of tasks, variants, and repetitions. Implementation details are in Appendix A.

When reporting aggregate results across the 23 PMO tasks, we follow PMO and sum per-task metrics across tasks. Since all reported metrics are bounded in $[0, 1]$, the maximum achievable aggregate score is bound by 23.

Results: Table 1 compares the performance of the SEISMO variants to the baseline models. The variant without descriptions is included to later isolate the role of external task information. Here, we focus on the full SEISMO agent with task descriptions. Across all metrics, SEISMO achieves consistently better performance than all baselines. Summed over all 23 tasks, the top-1 AUC over 50 oracle calls is 19.85 for SEISMO, compared to 7.06 for the strongest baseline, corresponding to a $2.8\times$ improvement. For the sum of best scores after 50 oracle calls, SEISMO achieves a $2.6\times$ improvement (21.18 vs. 8.18). Even when compared using

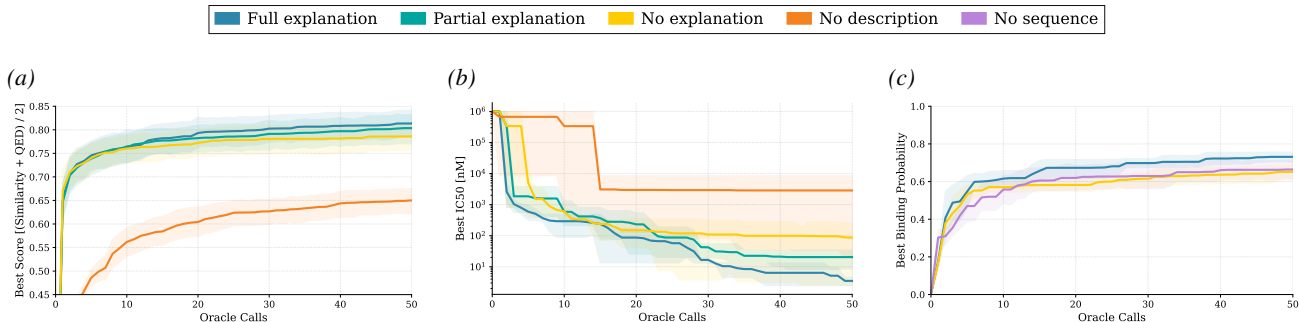


Figure 2. Panels (a–c) show best-so-far optimization curves under different oracle feedback variants. In (a), SEISMO optimizes structural similarity to randomly selected molecules together with drug-likeness (QED), averaged over 20 target molecules. Please note that the y-axis does not start at 0 to focus on the practically relevant score range. In (b), SEISMO performs inhibitory concentration (IC_{50}) optimization against SARS-CoV-2 M^{Pro} under novelty and drug-likeness constraints. Please note the logarithmic y-axis. In (c), SEISMO optimizes binding probability for a protein with no known binders using an expensive co-folding-based oracle. Shaded regions indicate 95% confidence intervals over repeated runs.

Table 1. Aggregate performance on the Practical Molecular Optimization (PMO) benchmark, summed over the 23 tasks. We report the sum of top-1 AUC after 50 oracle calls, the sum of top-1 AUC over 10,000 oracle calls, and the sum of the best scores achieved after 50 oracle calls. For the 10,000-call metric, SEISMO only optimizes during the first 50 oracle calls, and its best-so-far score is held fixed thereafter, while all baselines continue optimizing for the full 10,000 calls.

MODEL	SUM OF TOP-1 AUCS 50 ORACLE CALLS \uparrow	SUM OF TOP-1 AUCS 10000 ORACLE CALLS \uparrow	SUM OF BEST SCORE 50 ORACLE CALLS \uparrow
SEISMO	19.85 $^{+0.41}_{-0.38}$	21.17 $^{+0.59}_{-0.56}$	21.18 $^{+0.59}_{-0.56}$
SEISMO _{No Desc.}	8.50 $^{+0.83}_{-0.78}$	10.44 $^{+0.91}_{-1.10}$	10.45 $^{+0.91}_{-1.10}$
REINVENT	7.06 $^{+0.51}_{-0.43}$	14.74 $^{+0.95}_{-0.50}$	8.06 $^{+0.88}_{-0.62}$
GRAPH GA	7.04 $^{+0.49}_{-0.42}$	14.38 $^{+0.45}_{-0.48}$	8.18 $^{+0.55}_{-0.48}$
GP BO	6.95 $^{+0.34}_{-0.31}$	13.83 $^{+0.56}_{-0.60}$	8.00 $^{+0.53}_{-0.48}$

Table 2. Top-10 AUC over 1,000 oracle calls on the Practical Molecular Optimization (PMO) benchmark, summed over 23 tasks. Baseline results are taken from prior work (Nguyen & Grover, 2024). SEISMO proposes molecules only during the first 50 oracle calls, after which its top-10 score is held fixed, while all baselines continue optimizing for the full 1,000 calls.

MODEL	SUM OF AUC'S
SEISMO	20.24
LICO	11.71
MOLLEO	11.65
GENETIC GFN	11.56
GP BO	11.27
GRAPH GA	10.90
AUGMENTED MEMORY	10.81
REINVENT	10.68
SEISMO _{No Desc.}	9.91

the top-1 AUC over 10,000 oracle calls, SEISMO achieves a $1.4\times$ improvement, despite being restricted to 50 oracle calls compared to the full budget for the baselines.

Examining individual tasks rather than aggregate metrics reinforces this pattern. Across both metrics evaluated over 50 oracle calls, SEISMO achieves the best performance on all 23 tasks (cf. Tables D1 and D3). Over 10,000 oracle calls,

SEISMO remains best on 20 of the 23 tasks (cf. Table D2). Inspecting best scores after 50 oracle calls at the task level shows that SEISMO already reaches scores within 10% of the task maximum (≥ 0.9) on 16 of 23 tasks (cf. Table D3). Notably, this occurs within a number of oracle calls that is comparable to typical initial batch or population sizes used by prior methods, which have to evaluate multiple candidates before any update step can be taken. Consequently, SEISMO often reaches near-optimal solutions before such methods are able to perform their first optimization step.

The extended benchmark results, including recent LLM-based methods, can be found in Table 2. SEISMO again achieves the highest aggregate performance, improving the best score by a factor of 1.7. At the level of individual tasks, SEISMO is the best-performing model on 22 of the 23 tasks (see Table D4).

5.2. Impact of Information Level on Sample Efficiency

Setup: We evaluate the sample efficiency of SEISMO under varying amounts of available information:

No description: scalar score

Table 3. Model performance of variants with different levels of task and oracle information on three optimization tasks: (i) IC₅₀-QED-NOVEL optimization for SARS-CoV-2 M^{PRO}, reported as the AUC of the best constraint-fulfilling IC₅₀ over 50 oracle calls (lower is better); (ii) similarity-QED optimization over 20 random molecules, reported as top-1 AUC (higher is better); and (iii) similarity-QED optimization starting from Quercetin, reported as the number of oracle calls required to reach a fixed target score (lower is better).

MODEL VARIANT	IC ₅₀ -QED-NOVEL SARSCOV2M ^{PRO} TOP1 AUC ↓	SIM-QED 20 MOLECULES TOP1 AUC ↑	SIM-QED QUERCETIN ORACLE CALLS TO REACH TARGET SCORE ↓
FULL EXPLANATION	40187 ⁺¹² ₋₁₃	0.77 ^{+0.03} _{-0.03}	5.33 ^{+2.67} _{-2.33}
PARTIAL EXPLANATION	47068 ⁺¹³⁷⁰⁶ ₋₆₈₆₉	0.76 ^{+0.02} _{-0.03}	5.67 ^{+1.00} _{-1.07}
NO EXPLANATION	60611 ⁺³⁹⁶⁹⁴ ₋₂₀₄₆₈	0.75 ^{+0.03} _{-0.03}	12.00 ^{+7.00} _{-8.00}
NO DESCRIPTION	176184 ⁺¹²³⁸⁹⁷ ₋₁₄₇₈₅₅	0.58 ^{+0.02} _{-0.03}	> 50

No explanation: scalar score + subscores + task description

Partial explanation: scalar score + subscores + task description + explanation of one sub-score

Full explanation: scalar score + subscores + task description + explanations for all sub-scores

In the *no description* mode, the initial prompt only specifies that the model should optimize a score. In all other modes, the task is stated explicitly (cf. Figure 1).

We evaluate on two tasks reflecting common drug discovery settings: (i) hit identification, which involves discovering active molecules for a target protein, and (ii) lead optimization, which focuses on finding close analogs under additional constraints (More details in Appendix A).

For the hit identification proxy, we use the predicted inhibitory concentration (IC₅₀) against the SARS-CoV-2 main protease (M^{PRO}) as the main objective, where lower values indicate stronger inhibition. The final oracle (IC₅₀-QED-NOVEL) also includes novelty and drug-likeness constraints to restrict the search to chemically plausible and marketable molecules.

We evaluate sample efficiency using the optimization curve defined as the best feasible prediction so far over oracle calls, where feasibility is defined by satisfying the imposed drug-likeness and novelty constraints. Specifically, the curve records the lowest predicted inhibitory concentration among feasible molecules at each oracle call, and we quantify performance by the area under this constraint-filtered curve (AUC) over 50 oracle calls. Because this is a minimization task with unbounded scores, the resulting AUC is not normalized, with lower values indicating more sample-efficient optimization.

For the lead-optimization proxy, we study a similarity-constrained optimization task in which the agent seeks close analogs of a reference molecule with improved drug-likeness (Sim-QED). The scalar objective combines similarity to the reference and drug-likeness into a single score. We evaluate this task in two regimes: (i) a praxis-motivated case study using Quercetin as the reference molecule, which has known medicinal relevance but poor drug-like properties

(Gugler et al., 1975), and (ii) a randomized setting with 20 diverse reference molecules sampled to test robustness on targets with low a priori familiarity to the LLM.

We report top-1 AUC over 50 iterations for the scalar objective combining similarity and drug-likeness, averaged across target molecules. For the Quercetin case study, we report a goal-based metric: the number of oracle calls required to first reach a predefined target score corresponding to a close analog with improved drug-likeness (cf. Appendix A).

Depending on the mode, the oracle additionally returns an explanation of the score. Explanations for QED and Similarity provide property-level and substructure-level decompositions, respectively. For predicted IC₅₀ values, we use the feature attribution method SHAP. See Appendix E.3 for example explanations. In the partial explanation mode, only the drug-likeness QED score is being explained. We run SEISMO for 50 iterations in all four workflow modes for each task. All results are reported with 95% confidence intervals computed via bootstrap resampling.

Results: As shown in Table 3, the *no description* variant performs consistently worse than all other for both hit-identification and lead-optimization proxies, a pattern that is consistent with the PMO benchmark results across all metrics (Tables 1 and 2). This shows that knowledge of the optimization objective, within the initial prompt, is critical for effective LLM-driven optimization, as it enables the agent to condition its molecular proposals on task-relevant information available in the pretrained model.

We next analyze the effect of explanatory feedback beyond the task description. As shown in Table 3, increasing the level of explanatory feedback leads to a clear and consistent improvement in sample efficiency across all tasks and experimental settings. These results show that, beyond knowing what to optimize, providing feedback about why a molecule achieved a given score helps the agent identify how specific structural changes affect the objective, guiding the optimization process more effectively.

The optimization curves in Figures 2(a) and 2(b) clarify how this information is used. The benefit of a task description

is dominant and apparent throughout optimization, whereas the advantages of richer explanations emerge more gradually. Early performance is similar across explanation levels, but variants with richer feedback increasingly outperform those with less information as more oracle calls are made, highlighting the growing impact of explanatory feedback over time.

Beyond relative ordering between variants, the absolute values in Figures 2(a) and 2(b) show that SEISMO reaches chemically meaningful solutions within a small oracle budget. For the lead-optimization proxy, variants with task descriptions reach average similarity and drug-likeness values around 0.8 across 20 random reference molecules within 50 oracle calls, indicating close, drug-like analogs. For the hit-identification proxy, the full-explanation variant reliably identifies novel, drug-like molecules with predicted IC_{50} below 10 nM within the same budget, demonstrating convergence to strong target inhibition rather than modest score improvements.

5.3. Co-folding-based oracle

Setup: This oracle uses a so-called co-folding model to produce an evaluation function. A co-folding model (Abramson et al., 2024; Passaro et al., 2025; Corley et al., 2025) can take protein sequences, small compounds as SMILES and other biologically relevant molecules as inputs and produce a 3D representation (also called a structure) of the complex made up of the molecules. A special case in the co-folding space is the Boltz-2 model (Passaro et al., 2025), which built a so-called binding affinity prediction head on top of the structure prediction, which estimates how strong a small molecule will bind to a given protein. We employ the output of the affinity head as our score to guide the LLM to generate molecules keeping the protein sequence fixed. We randomly select a protein sequence from the MGnify metagenomics database (Richardson et al., 2023) that lies in a low-density region of the ESMAtlas embedding space (Lin et al., 2023), while still having a high-confidence predicted 3D structure. The chosen protein is MGY001550541752. These restrictions were chosen to challenge our agent: We wanted a protein with no known binders to reduce the chance of memorization by the LLM while at the same time still having a confident 3D structure for reliable Boltz-2 performance.

Similar to the previous experiments, the co-folding-based oracle was evaluated with three feedback conditions:

No sequence: we provided the Boltz-2 binding affinity probability together with a task description, but without the protein sequence of the target.

No explanation: as before, but the LLM has access to the protein sequence.

Full explanation: in addition to the previous information, the oracle provides the three-letter-codes of all residues that

are closer than 5Å to the molecule together with Boltz-2’s confidence scores (cf. Appendix C and E.3).

In Appendix C, we evaluate SEISMO on a well-studied (SARS-CoV-2 M^{Pro}) and a challenging target (TRIB2 pseudokinase), with abundant and limited known reference binders, respectively. In addition, we report ablations of the co-folding-based oracle.

Results: All three oracle feedback variants using the Boltz-2 oracle highlight that the LLM can use the binding affinity probability as a signal to optimize molecules. At the same time, the mean score never passes 0.75, which indicates that the agent is unable to identify a strong binder. Nevertheless, the results show that the agent can optimize for novel binders using expensive, but expressive oracles. As depicted in Figure 2(c), the added explanation (blue curve) leads to faster optimization compared to no explanation and no protein sequence. Interestingly, the optimization curves for the latter two cases are nearly indistinguishable, suggesting that for this protein, the protein sequence alone is not enough to help the agent improve the molecules more sample-efficiently.

6. Discussion

This work introduced SEISMO, a goal-directed LLM agent that performs inference-time optimisation by leveraging the chemical and biological priors encoded in large language models to navigate chemical space. Unlike population-based or batched acquisition methods, SEISMO operates in a strictly online loop, where every oracle call is immediately incorporated into the next proposal. This removes the sample-efficiency limits imposed by methods that must first evaluate an entire batch or population before any learning can occur. On the PMO benchmark, this design yields large gains in sample efficiency. SEISMO reaches near-optimal scores within 50 oracle calls and achieves 2–3× higher AUC than established baselines, even when those baselines are allowed to continue optimising for thousands of additional evaluations.

A central finding is that SEISMO’s sample efficiency depends on the type and amount of information provided to the agent. SEISMO integrates three types of information: natural-language objective descriptions, oracle scores, and, when available, explanations of those scores. Our ablations isolate the contribution of each component. When SEISMO receives only a scalar score without a task description, performance collapses across PMO and all case studies. Providing a task description leads to a dramatic improvement, demonstrating that the agent actively exploits prior chemical and biological knowledge encoded in the LLM to interpret the objective and propose meaningful starting molecules and molecular changes. However when using our co-folding or-

acle, providing the protein sequence alone does not improve method performance. One reason might be that the LLM does not know and cannot guess the correct binding site for this unfamiliar protein. Hence, limiting the use of sequence information alone. This theory is further strengthened by the observation that providing close residues as feedback improves performance. Consistent with this, adding explanations for why a molecule received a given score improves sample efficiency across all investigated tasks. This result has a broader implication: post-hoc explainability methods can be used not only for human-centred model interpretation, but as a machine-understood control signal that directly guides optimisation. In SEISMO, these explanations turn opaque oracle evaluations into actionable feedback about structure–property relationships, enabling more efficient and targeted search.

A few other recent methods incorporate LLMs into molecular optimisation. They are using the LLM as a component inside an evolutionary algorithm though to propose mutation or crossover candidates (Wang et al., 2024; Nguyen & Grover, 2024). In these approaches, the LLM does not maintain an explicit record of the optimisation trajectory. Our results show that this is an inefficient way to use LLMs. In such schemes, the LLM is blind to the optimisation trajectory and therefore cannot reason about cause and effect across iterations. SEISMO instead uses the LLM as the optimiser itself: the model conditions on the task specification and the full history of oracle feedback to make each successive proposal, enabling genuinely sequential decision-making. This allows SEISMO to reach strong solutions within minimal oracle calls.

Due to the fact, that LLM inference is computationally expensive, SEISMO is not optimized for settings with very low-cost oracles where millions of evaluations are feasible. Instead, it excels in regimes where each oracle call is costly, so that reducing the number of oracle calls dominates the LLM compute.

A second implication of conditioning on the full optimisation trajectory is that the effective optimisation horizon is bounded by the LLM’s context window. For all tasks considered in this work, this never became a limiting factor, though it may matter in very long-horizon settings. History summarisation could mitigate this limitation, but we do not explore it here.

We want to emphasize that practically relevant drug-discovery problems are not tabula rasa optimisation tasks. They are strongly structured by prior physical and chemical knowledge. Small-molecule binding is governed by hydrogen bonding, electrostatics, hydrophobicity, desolvation, and conformational strain, which sharply constrain which molecular modifications can plausibly improve affinity. These principles induce strong inductive biases over

chemical space, ruling out large classes of unproductive or physically implausible changes. Decades of medicinal-chemistry research have further established generalizable relationships between molecular structure and properties such as potency, selectivity, solubility, permeability, and metabolic stability. An optimiser that ignores this accumulated knowledge must rediscover these regularities from scratch, which is fundamentally sample-inefficient. SEISMO explicitly leverages this prior knowledge through the pretrained LLM, allowing it to start the search in chemically meaningful regions of the space and to propose edits that are aligned with known structure–property trends.

Nevertheless, relying on prior knowledge raises the question of how SEISMO behaves when such knowledge is limited or unavailable. We therefore evaluated the method on three settings designed to reduce the usefulness of memorized target-specific information: similarity and drug-likeness optimisation to 20 random molecules, SARS-CoV-2 M^{PRO} inhibitor discovery under a novelty constraint, and optimisation for binding to a novel protein with no known ligands. Across all three cases, SEISMO still exhibits strong optimisation behaviour. It identifies highly similar molecules with substantially improved drug-likeness, proposes novel SARS-CoV-2 M^{PRO} inhibitors with high predicted IC₅₀ values, and substantially increases the binding probabilities for a protein with no known binders. This indicates that SEISMO primarily exploits general chemical and biophysical priors rather than relying on memorized examples of specific targets.

SEISMO requires no training, no fine-tuning, and no hyperparameter tuning by the user. It combines pretrained domain knowledge from the LLM with information extracted from oracle calls via post-hoc explainability, yielding an optimiser that is easily usable in new tasks. Because SEISMO directly builds on general-purpose LLM capabilities, and those capabilities continue to improve, the method is expected to scale naturally with model progress. As LLMs become better at chemical reasoning, causal inference, and long-horizon planning, the same optimisation framework should become correspondingly more powerful without changing the underlying algorithm.

7. Conclusion

We introduced SEISMO, a goal-directed LLM agent that performs strictly online, inference-time molecular optimization by leveraging chemical and biological priors encoded in large language models. Across the PMO benchmark and additional medicinal-chemistry tasks, SEISMO achieves substantially higher sample efficiency than established optimization methods, often reaching near-optimal solutions within a few dozen oracle calls. Our ablations show that providing richer task-relevant information, via objective descriptions

and feedback beyond scalar scores, drives more sample-efficient exploration of chemical space. Together, these results position information-aware, trajectory-conditioned LLM agents as a practical framework for molecular optimization in regimes where oracle evaluations are expensive.

Impact Statement

This work introduces an LLM-based agent for molecular optimization that achieves substantially higher sample efficiency than existing approaches. In many realistic molecular design settings, each evaluation corresponds to an expensive or rate-limited computation or experiment, making the number of oracle calls the central bottleneck. By converging to high-quality solutions within a small number of evaluations, the proposed method directly addresses this bottleneck. As a result, the approach has strong relevance for early-stage drug discovery and other molecular design workflows, where careful use of resources is essential.

The proposed approach is designed as a decision-support tool rather than an autonomous discovery system and relies on externally defined evaluation oracles. Any real-world application would therefore remain subject to domain expertise, experimental validation, and regulatory oversight. While the method could in principle be applied to optimizing molecules with undesirable or harmful properties, this risk is not unique to the approach and is shared by existing molecular optimization techniques. In practice, such risks are mitigated through controlled access to evaluation oracles and established institutional safeguards. We do not identify ethical concerns beyond those already well established in machine learning-based molecular design.

Data Availability

The code is available at [GitHub](#).

References

- Abramson, J., Adler, J., Dunger, J., Evans, R., Green, T., Pritzel, A., Ronneberger, O., Willmore, L., Ballard, A. J., Bambrick, J., et al. Accurate structure prediction of biomolecular interactions with alphafold 3. *Nature*, 630 (8016):493–500, 2024.
- Bickerton, G. R., Paolini, G. V., Besnard, J., Muresan, S., and Hopkins, A. L. Quantifying the chemical beauty of drugs. *Nature chemistry*, 4(2):90–98, 2012.
- Boby, M. L., Fearon, D., Ferla, M., Filep, M., Koekemoer, L., Robinson, M. C., Consortium[‡], T. C. M., Chodera, J. D., Lee, A. A., London, N., von Delft, A., von Delft, F., Achdout, H., Aimon, A., Alonzi, D. S., Arbon, R., Aschenbrenner, J. C., Balcomb, B. H., Bar-David, E., Barr, H., Ben-Shmuel, A., Bennett, J., Bilenko, V. A., Borden, B., Boulet, P., Bowman, G. R., Brewitz, L., Brun, J., BVNBS, S., Calmiano, M., Carbery, A., Carney, D. W., Cattermole, E., Chang, E., Chernyshenko, E., Clyde, A., Coffland, J. E., Cohen, G., Cole, J. C., Contini, A., Cox, L., Croll, T. I., Cvitkovic, M., Jonghe, S. D., Dias, A., Donckers, K., Dotson, D. L., Douangamath, A., Duberstein, S., Dudgeon, T., Dunnett, L. E., Eastman, P., Erez, N., Eyermann, C. J., Fairhead, M., Fate, G., Fedorov, O., Fernandes, R. S., Ferrins, L., Foster, R., Foster, H., Fraisse, L., Gabizon, R., García-Sastre, A., Gawriljuk, V. O., Gehrtz, P., Gileadi, C., Giroud, C., Glass, W. G., Glen, R. C., Glinert, I., Godoy, A. S., Gorichko, M., Gorrie-Stone, T., Griffen, E. J., Haneef, A., Hart, S. H., Heer, J., Henry, M., Hill, M., Horrell, S., Huang, Q. Y. J., Huliak, V. D., Hurley, M. F. D., Israely, T., Jajack, A., Jansen, J., Jnoff, E., Jochmans, D., John, T., Kaminow, B., Kang, L., Kantsadi, A. L., Kenny, P. W., Kiappes, J. L., Kinakh, S. O., Kovar, B., Krojer, T., La, V. N. T., Laghimi-Hahn, S., Lefker, B. A., Levy, H., Lithgo, R. M., Logvinenko, I. G., Lukacik, P., Macdonald, H. B., MacLean, E. M., Makower, L. L., Malla, T. R., Marples, P. G., Matviiuk, T., McCorkindale, W., McGovern, B. L., Melamed, S., Melnykov, K. P., Michurin, O., Miesen, P., Mikolajek, H., Milne, B. F., Minh, D., Morris, A., Morris, G. M., Morwitzer, M. J., Moustakas, D., Mowbray, C. E., Nakamura, A. M., Neto, J. B., Neyts, J., Nguyen, L., Noske, G. D., Oleinikovas, V., Oliva, G., Overheul, G. J., Owen, C. D., Pai, R., Pan, J., Paran, N., Payne, A. M., Perry, B., Pingle, M., Pinjari, J., Politi, B., Powell, A., Pšenák, V., Pulido, I., Puni, R., Rangel, V. L., Reddi, R. N., Rees, P., Reid, S. P., Reid, L., Resnick, E., Ripka, E. G., Robinson, R. P., Rodriguez-Guerra, J., Rosales, R., Rufa, D. A., Saar, K., Saikatendu, K. S., Salah, E., Schaller, D., Scheen, J., Schiffer, C. A., Schofield, C. J., Shafeev, M., Shaikh, A., Shaqra, A. M., Shi, J., Shurrush, K., Singh, S., Sittner, A., Sjö, P., Skyner, R., Smalley, A., Smeets, B., Smilova, M. D., Solmesky, L. J., Spencer,

- J., Strain-Damerell, C., Swamy, V., Tamir, H., Taylor, J. C., Tennant, R. E., Thompson, W., Thompson, A., Tomásio, S., Tomlinson, C. W. E., Tsurupa, I. S., Tumber, A., Vakonakis, I., van Rij, R. P., Vangeel, L., Varghese, F. S., Vaschetto, M., Vitner, E. B., Voelz, V., Volkamer, A., Walsh, M. A., Ward, W., Weatherall, C., Weiss, S., White, K. M., Wild, C. F., Witt, K. D., Wittmann, M., Wright, N., Yahalom-Ronen, Y., Yilmaz, N. K., Zaidmann, D., Zhang, I., Zidane, H., Zitzmann, N., and Zvornicanin, S. N. Open science discovery of potent noncovalent sars-cov-2 main protease inhibitors. *Science*, 382(6671), 2023.
- Bohacek, R. S., McMartin, C., and Guida, W. C. The art and practice of structure-based drug design: a molecular modeling perspective. *Medicinal research reviews*, 16(1): 3–50, 1996.
- Bran, A. M., Cox, S., Schilter, O., Baldassari, C., White, A. D., and Schwaller, P. Augmenting large language models with chemistry tools. *Nature Machine Intelligence*, 6(5):525–535, 2024.
- Chen, T. Xgboost: A scalable tree boosting system. *Cornell University*, 2016.
- Corley, N., Mathis, S., Krishna, R., Bauer, M. S., Thompson, T. R., Ahern, W., Kazman, M. W., Brent, R. I., Didi, K., Kubaney, A., et al. Accelerating biomolecular modeling with atomworks and rf3. *bioRxiv*, 2025. doi: 10.1101/2025.08.14.670328.
- Durant, J. L., Leland, B. A., Henry, D. R., and Nourse, J. G. Reoptimization of mdl keys for use in drug discovery. *Journal of chemical information and computer sciences*, 42(6):1273–1280, 2002.
- Foulkes, D. M., Byrne, D. P., Yeung, W., Shrestha, S., Bailey, F. P., Ferries, S., Eyers, C. E., Keeshan, K., Wells, C., Drewry, D. H., Zuercher, W. J., Kannan, N., and Eyers, P. A. Covalent inhibitors of egfr family protein kinases induce degradation of human tribbles 2 (trib2) pseudokinase in cancer cells. *Science Signaling*, 11(549), 2018.
- Gao, W., Fu, T., Sun, J., and Coley, C. Sample efficiency matters: a benchmark for practical molecular optimization. *Advances in neural information processing systems*, 35:21342–21357, 2022.
- Ghiandoni, G. M., Evertsson, E., Riley, D. J., Tyrchan, C., and Rathi, P. C. Augmenting dmta using predictive ai modelling at astrazeneca. *Drug discovery today*, 29(4): 103945, 2024.
- Gugler, R., Leschik, M., and Dengler, H. Disposition of quercetin in man after single oral and intravenous doses. *European journal of clinical pharmacology*, 9(2):229–234, 1975.
- Guo, J. and Schwaller, P. Beam enumeration: probabilistic explainability for sample efficient self-conditioned molecular design. *arXiv preprint arXiv:2309.13957*, 2023.
- Guo, J. and Schwaller, P. Augmented memory: sample-efficient generative molecular design with reinforcement learning. *Jacs Au*, 4(6):2160–2172, 2024.
- Huang, K., Fu, T., Gao, W., Zhao, Y., Roohani, Y., Leskovec, J., Coley, C., Xiao, C., Sun, J., and Zitnik, M. Therapeutics data commons: Machine learning datasets and tasks for drug discovery and development. In Vanschoren, J. and Yeung, S. (eds.), *Proceedings of the Neural Information Processing Systems Track on Datasets and Benchmarks*, volume 1, 2021.
- Inoue, Y., Song, T., Wang, X., Luna, A., and Fu, T. Drugagent: Multi-agent large language model-based reasoning for drug-target interaction prediction. In *ICLR 2025 Workshop on Machine Learning for Genomics Explorations*, 2025.
- Jensen, J. H. A graph-based genetic algorithm and generative model/monte carlo tree search for the exploration of chemical space. *Chemical science*, 10(12):3567–3572, 2019.
- Kim, S., Chen, J., Cheng, T., Gindulyte, A., He, J., He, S., Li, Q., Shoemaker, B. A., Thiessen, P. A., Yu, B., et al. Pubchem 2025 update. *Nucleic acids research*, 53(D1): D1516–D1525, 2025.
- Kunzmann, P., Müller, T. D., Greil, M., Krumbach, J. H., Anter, J. M., Bauer, D., Islam, F., and Hamacher, K. Biotite: new tools for a versatile python bioinformatics library. *BMC bioinformatics*, 24(1):236, 2023.
- LangChain AI. Langgraph: Stateful, multi-agent llm workflows. <https://github.com/langchain-ai/langgraph>, 2025. Version 1.0.5. Accessed: 2026-01-08.
- Lin, Z., Akin, H., Rao, R., Hie, B., Zhu, Z., Lu, W., Smetanin, N., Verkuil, R., Kabeli, O., Shmueli, Y., et al. Evolutionary-scale prediction of atomic-level protein structure with a language model. *Science*, 379(6637): 1123–1130, 2023.
- Lipinski, C. A., Lombardo, F., Dominy, B. W., and Feeney, P. J. Experimental and computational approaches to estimate solubility and permeability in drug discovery and development settings. *Advanced drug delivery reviews*, 64:4–17, 2012.
- Lundberg, S. M. and Lee, S.-I. A unified approach to interpreting model predictions. *Advances in neural information processing systems*, 30, 2017.

- McNaughton, A. D., Sankar Ramalaxmi, G. K., Krueel, A., Knutson, C. R., Varikoti, R. A., and Kumar, N. Cactus: Chemistry agent connecting tool usage to science. *ACS omega*, 9(46):46563–46573, 2024.
- Meli, R., Morris, G. M., and Biggin, P. C. Scoring functions for protein-ligand binding affinity prediction using structure-based deep learning: a review. *Frontiers in bioinformatics*, 2:885983, 2022.
- Nguyen, T. and Grover, A. Lico: Large language models for in-context molecular optimization. *arXiv preprint arXiv:2406.18851*, 2024.
- Olivecrona, M., Blaschke, T., Engkvist, O., and Chen, H. Molecular de-novo design through deep reinforcement learning. *Journal of cheminformatics*, 9(1):48, 2017.
- Pan, Q., Xu, D., Yao, J. X., Ma, L., Zhu, Z., and Ji, J. Frogent: An end-to-end full-process drug design agent. *arXiv preprint arXiv:2508.10760*, 2025.
- Passaro, S., Corso, G., Wohlwend, J., Reveiz, M., Thaler, S., Somnath, V. R., Getz, N., Portnoi, T., Roy, J., Stark, H., Kwabi-Addo, D., Beaini, D., Jaakkola, T., and Barzilay, R. Boltz-2: Towards accurate and efficient binding affinity prediction. *bioRxiv*, 2025. doi: 10.1101/2025.06.14.659707.
- Pedregosa, F., Varoquaux, G., Gramfort, A., Michel, V., Thirion, B., Grisel, O., Blondel, M., Prettenhofer, P., Weiss, R., Dubourg, V., Vanderplas, J., Passos, A., Cournapeau, D., Brucher, M., Perrot, M., and Duchesnay, E. Scikit-learn: Machine learning in Python. *Journal of Machine Learning Research*, 12:2825–2830, 2011.
- RDKit. Rdkit: Open-source cheminformatics. <https://www.rdkit.org>, 2025. Release_2025_09_3.
- Richardson, L., Allen, B., Baldi, G., Beracochea, M., Bileschi, M. L., Burdett, T., Burgin, J., Caballero-Pérez, J., Cochrane, G., Colwell, L. J., et al. Mgnify: the microbiome sequence data analysis resource in 2023. *Nucleic acids research*, 51(D1):D753–D759, 2023.
- Solovev, G. V., Zhidkovskaya, A. B., Orlova, A., Gubina, N., Vepreva, A., Golovinskii, R., Tonkii, I., Dubrovsky, I., Gurev, I., Gilemkanov, D., et al. Madd: Multi-agent drug discovery orchestra. In *Findings of the Association for Computational Linguistics: EMNLP 2025*, pp. 6956–6998, 2025.
- Tang, X., Hu, T., Ye, M., Shao, Y., Yin, X., Ouyang, S., Zhou, W., Lu, P., Zhang, Z., Zhao, Y., et al. Chema-gent: Self-updating memories in large language models improves chemical reasoning. In *The Thirteenth International Conference on Learning Representations*, 2025.
- Tripp, A., Simm, G. N., and Hernández-Lobato, J. M. A fresh look at de novo molecular design benchmarks. In *NeurIPS 2021 AI for Science Workshop*, 2021.
- Wang, H., Skreta, M., Ser, C.-T., Gao, W., Kong, L., Strieth-Kalthoff, F., Duan, C., Zhuang, Y., Yu, Y., Zhu, Y., et al. Efficient evolutionary search over chemical space with large language models. *arXiv preprint arXiv:2406.16976*, 2024.
- Weininger, D. Smiles, a chemical language and information system. 1. introduction to methodology and encoding rules. *Journal of Chemical Information and Computer Sciences*, 28(1):31–36, 1988.
- Wognum, C., Ash, J. R., Aldeghi, M., Rodríguez-Pérez, R., Fang, C., Cheng, A. C., Price, D. J., Clevert, D.-A., Engkvist, O., and Walters, W. P. A call for an industry-led initiative to critically assess machine learning for real-world drug discovery. *Nature Machine Intelligence*, 6(10):1120–1121, 2024.

A. Implementation Details

Agent Architecture. We implement our molecule optimization agent as a cyclic workflow using LangGraph (LangChain AI, 2025). Our workflow consists of five nodes: generation, parsing, validation, prediction, and finalisation. The conversation history begins with a system prompt providing general instructions (cf. Appendix E.1) followed by a task-specific first message describing the optimization objective (cf. Appendix E.2). At each iteration, the generation node invokes an LLM with this full history and instructs it to output structured JSON containing a SMILES string (Weininger, 1988) and rationale. The parsing node extracts the JSON, and the validation node uses RDKit (RDKit, 2025) to verify SMILES validity. Invalid outputs trigger a re-generation with corrective feedback; we count these as iterations to avoid infinite loops. Valid molecules proceed to the prediction node, where a pluggable oracle computes a score and optionally an explanation. We then construct feedback including the score, iteration count, and any explanation-derived insights, which is appended to the conversation history for the next generation step. The loop terminates upon reaching a target score or an iteration limit. The finalisation node then generates a natural language summary of the optimization trajectory grounded in the structured per-step records (generated SMILES and rationales) and oracle scores. The summary highlights which structural modifications improved or degraded performance, aimed to help medicinal chemists interpret the agent’s reasoning and extract actionable insights. Unless stated otherwise, the generation and finalisation nodes use `claude-opus-4-5-20251101-v1:0` from Anthropic. We selected this LLM based on an ablation study (cf. Appendix B).

Oracle Instantiation and Benchmarking Protocol. The prediction node is implemented as a modular oracle interface. When switching between tasks, we only replace the oracle callable and the initial task message used to initialize the conversation history, while keeping the rest of the workflow unchanged. For head-to-head comparison with established molecule-optimization methods, we evaluate on the Practical Molecular Optimization (PMO) benchmark, which consists of 23 different molecule optimisation tasks and was designed to evaluate sample efficiency in molecular optimisation (Gao et al., 2022). The tasks span a diverse set of medicinal-chemistry objectives, including drug-likeness, bioactivity against targets, similarity- and rediscovery-based goals, isomer and substructure constraints, and multi-property optimization, and require optimizing molecular structures through oracle calls. To run our agent on PMO tasks, we call the benchmark oracles through the TDC package, following the same oracle access pattern used in the original PMO setup (Huang et al., 2021).

Importantly, to avoid altering the benchmark oracles, the oracle feedback provided to the agent is limited to the scalar score returned by the oracle without any further explanation of the score.

Within this constraint, we test two variants that differ in whether the LLM is told what the oracle measures in the description. In the *task described* variant, the initial task message explicitly states the objective (e.g., “maximize the geometric mean of ...”), while the per-iteration feedback still contains only the scalar score. Our descriptions of the tasks are comparable to the descriptions used in other work (Wang et al., 2024; Nguyen & Grover, 2024) and are specified in Appendix E.2 and our GitHub. In the *no description* variant, the initial message omits any description of the objective, so the agent must treat the oracle as fully black-box and rely purely on observed (molecule, score) pairs. For each of the 23 PMO tasks, we run both variants for 3 independent repetitions. Due to the API costs for LLM inference, we cap each run at 50 LLM calls.

We follow PMO’s recommended sample-efficiency evaluation via the area under the optimization curve (AUC) (Gao et al., 2022). The optimization curve is defined as the top- n score achieved so far versus the number of oracle calls; we focus on $n = 1$ (top-1) because we are interested in finding a high-scoring molecule rather than optimizing finding a batch of molecules in our setting (cf. problem formulation). We report top-1 AUC over the first 50 oracle calls, matching our agent’s optimization budget, and top-1 AUC over 10,000 oracle calls for consistency with PMO reporting (Gao et al., 2022). Our agent is only allowed to propose molecules for the first 50 oracle calls; for calls 51–10,000 we keep its best-so-far score fixed (no further optimization). In contrast, PMO baselines are evaluated over the full 10,000 oracle calls using their published trajectories. We also report the best score achieved after 50 oracle calls. We report 95% CIs that we computed via bootstrap resampling of the different repetitions across the 23 tasks.

To provide a broader comparison that also includes more recent models, we additionally evaluate top-10 AUC over 1,000 oracle calls and compare against the values reported by Nguyen et al., who provide results for a broad range of optimization models (Nguyen & Grover, 2024). For our agent, we stop optimization after 50 oracle calls and keep the top-10 score fixed for the remaining 950 iterations, whereas all other methods from Nguyen et al. were allowed to optimize for the full 1,000 oracle calls.

For baseline comparisons within the PMO benchmark, we use the released per-iteration trajectories (including the proposed SMILES and corresponding oracle scores) and recompute our metrics (top-1 AUC at 50 and 10,000 calls, and best-at-50) from those raw traces to ensure identical metric definitions. We include the top three methods reported by

PMO under their benchmark evaluation. In contrast, for the additional Nguyen et al. methods we only use their published top-10 AUC values, since they do not release the underlying per-iteration SMILES/oracle-call traces needed to compute our other metrics. Reproducing those traces would require rerunning their methods and would be prohibitively expensive due to LLM API costs.

Extended Tasks with Interpretable Oracle Feedback.

Beyond PMO, we evaluate the agent on two tasks that more directly mirror common medicinal-chemistry iteration loops: improving a predicted activity signal under a drug-likeness constraint, and improving drug-likeness while preserving similarity to a reference molecule. Since for these tasks we implement the oracles ourselves, we can also control the amount of explanation returned to the agent and ablate different feedback settings.

Hit-identification proxy: SARS-CoV-2 M^{pro} inhibition with a QED and novelty constraint. The objective is to minimise a predicted IC_{50} (the half-maximal inhibitory concentration) while satisfying $QED \geq 0.6$ (Quantitative Estimate of Drug-likeness). The oracle returns (i) a scalar optimisation score used by the agent and (ii) a structured breakdown containing the predicted IC_{50} and QED. Predicted IC_{50} is produced by an XGBoost regressor (Chen, 2016) trained on a dataset of measured IC_{50} values against SARS-CoV-2 main protease (training details are provided at the end of this part of the Appendix). Molecules are featurised using MACCS keys (Durant et al., 2002). QED is computed with RDKit (RDKit, 2025) and is a heuristic measure derived from the empirical distribution of molecular properties among approved oral drugs (Bickerton et al., 2012). This constraint additionally helps to keep the search in regions where the XGBoost predictor is more reliable. We additionally constrain on novelty, which we define as absence from PubChem (Kim et al., 2025); molecules that are present in PubChem are treated as non-novel and are considered invalid proposals. In the task description we refer only to a generic protease target (rather than explicitly naming SARS-CoV-2 M^{pro}), since explicitly naming the target triggered LLM refusal behaviour due to its safety filters.

Lead-optimisation proxy: Similarity to a reference molecule with improved QED. Given a reference molecule x^* , the goal is to maximise structural similarity to x^* while increasing QED. Similarity is computed as Tanimoto similarity between MACCS-key fingerprints of x^* and the proposed molecule (Durant et al., 2002); QED is computed with RDKit (RDKit, 2025). The oracle returns both sub-scores (sim, QED) and a scalar objective defined as their average $s = \frac{1}{2}(\text{sim} + \text{QED})$, which is the quantity optimized by the agent. Consequently, $s \geq 0.8$ corresponds to an average similarity and QED of at least 0.8.

We study two scenarios for this task. (i) A praxis-motivated case study with $x^* = \text{Quercetin}$, which has been discussed as a potential therapeutic but is known for poor solubility/bioavailability and rapid metabolism. The aim is to find close analogs with improved drug-like characteristics. (ii) A setting intended to evaluate the performance on molecules with low a priori familiarity to the LLM: we sample 20 target molecules uniformly at random from PubChem under constraints designed to ensure diversity and a non-trivial QED-improvement problem. Concretely, each sampled target has molecular weight < 500 , $QED \leq 0.5$, and maximum pairwise Tanimoto similarity ≤ 0.2 with all previously selected targets (cf. Figure A1).

Oracle explanations. For the XGBoost IC_{50} model, explanations are generated with SHAP (Lundberg & Lee, 2017) over MACCS keys, yielding per-feature attributions indicating which substructures most increased or decreased the predicted IC_{50} . We present the 10 substructures with highest attribution (driving lower IC_{50}) and the 10 with lowest attribution (driving higher IC_{50}), each annotated with its presence in the current molecule and SMARTS pattern to guide structural modifications. For QED, we provide a property-level decomposition (e.g., molecular weight, logP, HBD/HBA, PSA, rotatable bonds) and indicate which properties most reduced QED for the current proposal and what ranges would be more favourable. For similarity, we explain which MACCS keys differ between x^* and the proposal (keys present in exactly one of the two), and map these keys to their corresponding SMARTS patterns to make the structural mismatch interpretable. See Appendix E.3 for example explanations.

Evaluation protocol and metrics. For the SARS-CoV-2 M^{pro} task and the Quercetin lead-optimisation task, we run 3 independent repetitions for each of the four information conditions, for up to 50 iterations. For the 20 random PubChem targets, we run one 50-iteration optimisation per target and information condition, and report results averaged over the 20 targets.

For the SARS-CoV-2 M^{pro} task, we evaluate sample efficiency using the optimisation curve of the best (lowest) predicted IC_{50} among molecules that satisfy the constraints ($QED \geq 0.6$ and novel) versus oracle calls. If no molecule that satisfies the constraints has been found yet, we set the curve value to 1 mM to allow AUC computation. We report the AUC over 50 oracle calls under this constraint-filtered curve. For the 20 random-target lead-optimisation setting, we report top-1 AUC over 50 iterations for the scalar objective $s = \frac{1}{2}(\text{sim} + \text{QED})$, averaged across targets. Since we include Quercetin as a concrete example, we evaluate it with a more directly interpretable, goal-based metric: the number of oracle calls required to first reach $s \geq 0.8$ (i.e., average similarity and QED of at least 0.8), corresponding

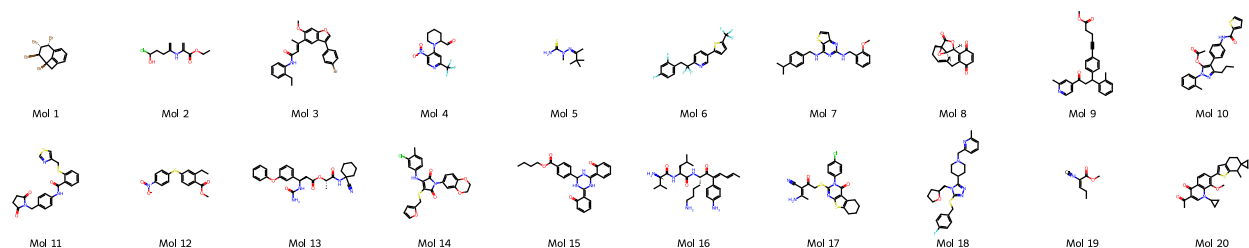


Figure A1. Visualisation of the 20 randomly sampled molecules from PubChem that were used as reference molecules in the lead optimisation proxy.

to finding a close analog with improved drug-like properties. For all tasks the 95% confidence intervals are computed via bootstrap resampling.

XGBoost training. The XGBoost regression model was implemented using the `xgboost` python package (version 3.1.2) and trained to predict pIC_{50} values for SARS-CoV-2 M^{pro} inhibition using the ASAP Discovery antiviral potency dataset (asap-discovery/antiviral-potency-2025-unblinded) accessed via the Polaris platform (Wognum et al., 2024). Molecular structures were encoded as 167-bit MACCS fingerprints using RDKit. The XGBRegressor was configured with 2,000 estimators, a learning rate of 0.03, subsample ratio of 0.8, L1 regularization ($\alpha = 0.1$), L2 regularization ($\lambda = 2$), histogram-based tree construction with loss-guided growth policy, and a maximum of 128 leaves per tree. Hyperparameter optimization was performed via random search over 40 trials, exploring combinations of maximum tree depth (3, 4, 5, 6), minimum child weight (1, 3, 5, 7), gamma (0, 0.1, 0.5, 1.0), and column subsampling ratio (0.4, 0.6, 0.8, 1.0). The model with the lowest root mean squared error (RMSE) on the held-out test set was selected as the final model.

Co-folding-based oracle. The co-folding-based oracle has access to the target protein sequence and receives a molecule proposal from the LLM in the form of a SMILES string (Weininger, 1988). These two inputs are passed to the Boltz-2 co-folding model. We invoke Boltz-2 with its default parameters, except that we store the predicted structure in the PDB format and do not pre-compute multiple sequence alignments (MSAs), but let Boltz-2 handle that via their default MSA-server. We run the model on an NVIDIA A100 GPU and give it a time limit of five minutes. If the time out is reached or the model process reports a non-zero exit code the oracle returns NaN as its score. On model success, the oracle extracts the binding affinity probability score (`affinity_probability_binary`), which is a sigmoid probability representing Boltz-2’s belief that the

compound binds to the protein. In addition, Boltz-2 provides a binding affinity value (`affinity_pred_value`), which aims to predict the affinity via the IC_{50} value of the system. We decided to use the probability as the oracle’s score, as the IC_{50} score is not normalized and preliminary experiments showed that the agent had difficulty optimizing it. If the oracle failed to parse the affinity scores, we again reported a NaN to the agent.

As an explanation, the oracle reported Boltz-2’s non-zero confidence scores and the protein’s residues that were close to the ligand. In particular, we reported Boltz-2’s aggregated confidence score (`confidence_score`), the (interface and ligand) predicted template modeling (TM) score (`[ligand_lig]ptm`), the (interface) predicted local distance difference test score (`complex_[i]plddt`), and the (interface) predicted distance error (`complex_[i]pde`). Close residues were defined as all residues which have at least one heavy atom (any non-hydrogen atom) that is no more than 5\AA away from a compound heavy atom. We used the biotite (Kunzmann et al., 2023) and scikit-learn (Pedregosa et al., 2011) libraries to compute these distances. We reported the three letter code and index of all residues in the protein sequence satisfying our closeness definition to the LLM. If any of the above computations failed, we reported an empty explanation.

B. LLM Ablation

We performed an ablation over multiple LLM backends on the 20 random-target similarity+QED task. We tested `claude-opus-4-5-20251101-v1:0`, `claude-sonnet-4-5-20250929-v1:0`, `gpt-4.1-2025-04-14`, `gpt-5.1-2025-11-13` with no reasoning, and `gpt-5.1-2025-11-13` with medium reasoning effort. We also evaluated DeepSeek-R1, but excluded it because it frequently failed to produce syntactically valid SMILES strings under our JSON-constrained output format. In this ablation, we swapped only the LLM while keeping prompts, JSON schema,

retry/validation logic, oracle, and the 50-iteration optimization budget fixed, and compared models by mean top-1 AUC over 50 iterations (averaged across the 20 targets) for $s = \frac{1}{2}(\text{sim} + \text{QED})$. We included gpt-5.1 only at medium reasoning effort because even this setting had long per-call reasoning times, and running high reasoning effort would have led to impractically long end-to-end runtimes given our experimental scale.

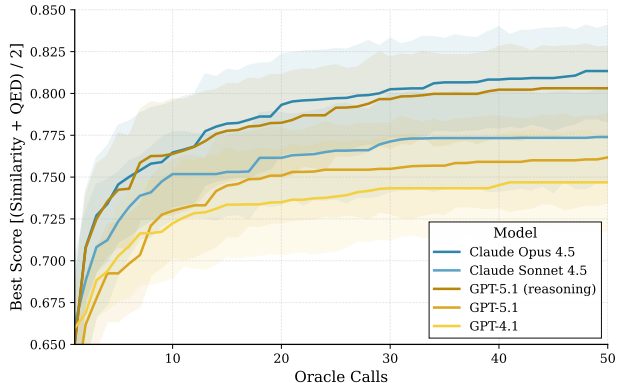


Figure B1. Comparison of multiple large language models on the 20 random-target similarity+QED task. The line and band denote mean and standard deviation respectively.

Averaged across targets, newer models achieved higher performance, with Claude Opus 4.5 achieving the best overall score, closely followed by GPT-5.1 with medium reasoning (Figure B1). In addition to its slightly better performance, Opus-4.5 exhibited faster response times and lower per-iteration costs than GPT-5.1 with medium reasoning under our API provider’s pricing and latency at the time of experimentation. Taken together, these results motivated our choice of Opus-4.5 for the experiments in this work. Figure B1 also shows that Opus-4.5 outperforms Sonnet-4.5 and GPT-5.1 outperforms GPT-4.1, indicating a correlation between general model capability and performance on our molecular optimisation task.

C. Further co-folding-based results

We performed three additional experiments to validate the co-folding-based oracle. First, we report the oracle performance on a well studied target (SARS-CoV-2 M^{pro}), highlighting that in this setting the agent requires less context information to find good binding candidates. Second, we compare SEISMO’s optimization curve for two protein targets to experimentally validated reference binders. Third, we perform ablation studies of the oracle to explore how the LLM exploits the oracle scores.

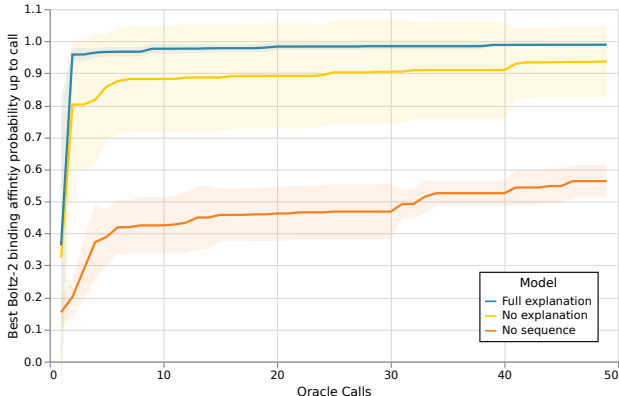


Figure C1. Optimization of a compound for binding affinity to SARS-CoV-2 M^{pro}. The line and band denote mean and standard deviation respectively, computed over five repeats for each model.

SARS-CoV-2 M^{pro} target. The SARS-CoV-2 main protease is a well-studied target with many known binders. As such, we expected this to be an easy setting for our agent as the LLM training data should cover example binders.

Indeed, Figure C1 shows that as soon as the LLM has access to the protein sequence, it can generate compounds with very high binding probability ($\geq 90\%$). If the oracle also returns an explanation (close residues and confidence scores), the agent reaches a close to optimal compound in the second iteration. It is also noteworthy that the “no explanation” models produced a high standard deviation, indicating that the LLM could not generate (near) optimal solutions as consistently as with the added context in the “full explanation” model. Hiding the protein sequence has a substantially detrimental effect on model performance.

Compared to the agent’s performance on MGY001550541752 (cf. Figure 2(c)), we see that in the SARS-CoV-2 case the “no explanation” optimization curve is closer to the “full explanation” curve while in the MGY001550541752 case the “no explanation” curve is almost indistinguishable from the “no protein” curve. We attribute this difference to the task difficulty: The sequence allows the LLM to identify the protein, which, in the SARS-CoV-2 case, enables the LLM to retrieve good binders from memory and use them as templates for its proposal. In the MGY001550541752 case, the sequence information is not enough as there are few if any known binders in the literature. Hence the performance only improves with additional context, helping the model to identify potential binding sights.

Comparison to known reference binders. In Figure C2, we evaluate the agent-generated candidate molecules relative to known reference binders reported in the literature for two representative targets: the well-characterized

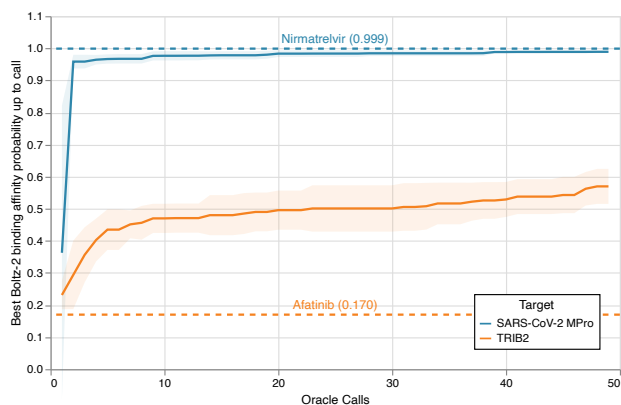


Figure C2. Comparison of predicted binding affinity between SEISMO-generated compounds and known reference ligands for an easy target (SARS-CoV-2 main protease, M^{Pro}) and a challenging target (TRIB2 pseudokinase). Dashed lines indicate the Boltz2-predicted binding probabilities of the reference compounds nirmatrelvir (M^{Pro}) and afatinib (TRIB2).

SARS-CoV-2 main protease (M^{Pro}) and the more challenging TRIB2 pseudokinase. For M^{Pro} , we use the clinically validated inhibitor nirmatrelvir (Boby et al., 2023) as a reference compound. In contrast, TRIB2 does not currently have a well-established high-affinity small-molecule ligand. However, several covalent kinase inhibitors, including afatinib (Foulkes et al., 2018), have been reported to interact with and destabilize TRIB2 in cellular and biochemical assays. We therefore adopt afatinib as a representative reference compound for this target.

For the M^{Pro} binding task, the highest-scoring molecule generated by the agent achieves a Boltz2-predicted binding probability of 0.995, compared to 0.999 for nirmatrelvir, indicating that the optimization process is able to recover candidates with predicted binding strength comparable to that of a well-established antiviral inhibitor. In the more challenging TRIB2 setting, SEISMO identifies a compound with a substantially higher predicted binding probability than the reference compound, achieving 0.633 versus 0.170 for afatinib.

While these results highlight the ability of our agent to propose promising candidate molecules for both well-studied and less-characterized protein targets, it is important to emphasize that these values only reflect Boltz2 predictions. Experimental validation, including direct binding and functional assays, would be required to determine whether the proposed compounds exhibit biological activity toward TRIB2 and other challenging targets.

Oracle ablations. With these experiments, we wanted to understand how the LLM weighs its own chemical knowledge as present in its training data against the external signal as provided by the oracle score and explanation. We again

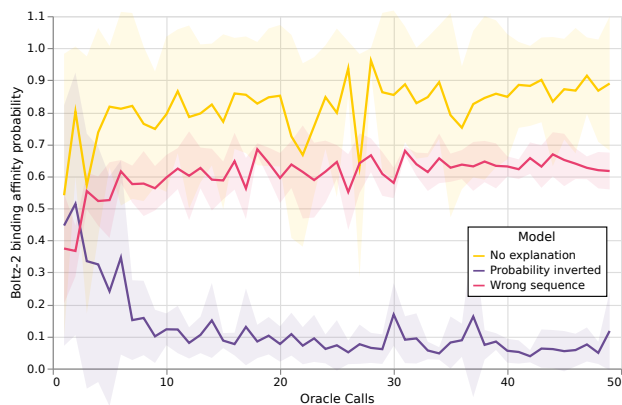


Figure C3. Binding probability over oracle call for SARS-CoV-2 M^{Pro} . The line and band denote mean and standard deviation respectively, computed over five repeats for each model.

used the SARS-CoV-2 main protease as the target protein and performed two ablations. First, we reported a wrong and irrelevant protein sequence to the LLM while still using the correct sequence for the Boltz-2 affinity predictions (“Wrong sequence”). We chose the green fluorescent protein (GFP) as the decoy protein. Second, we reported the correct sequence to the LLM, but inverted the Boltz-2 affinity score (“Probability inverted”). In both cases, we ran the oracle in “no explanation” mode. We compared these ablations to the pure “no explanation” mode as a baseline.

The results can be found in Figure C3. Please note that in contrast to Figure 2(c) and C1, we report the current mean Boltz-2 binding affinity probability score at each iteration — not the maximum score up to the given iteration. We chose this deviation to highlight the agent’s behavior in the “probability inverted” scenario.

In the “wrong protein” setup, the optimization curve still follows an upward trend indicating that the LLM tries to incorporate the oracle’s feedback. However, the mean binding probability never passes 70%, highlighting the difficulty of the agent to optimize the compound given the contradictory information. In the “inverted probability” setup, we see that the optimization curve consistently decreases, suggesting that the LLM puts more weight on the provided score than its internal knowledge.

D. Individual Task Scores for PMO

Table D1. Top1 AUC over 50 iterations. Performance comparison across molecular optimization tasks. Higher is better.

TASK	SEISMO	SEISMO _{No Desc.}	REINVENT	GRAPH GA	GP BO
ALBUTEROL_SIMILARITY	0.990±0.000	0.407±0.062	0.358±0.021	0.384±0.026	0.372±0.028
AMLODIPINE_MPO	0.882±0.001	0.465±0.009	0.432±0.033	0.425±0.019	0.430±0.035
CELECOXIB_REDISCOVERY	0.990±0.000	0.386±0.025	0.262±0.036	0.258±0.021	0.250±0.013
DECO_HOP	0.934±0.017	0.568±0.002	0.558±0.008	0.801±0.009	0.803±0.008
DRD2	0.990±0.000	0.432±0.418	0.195±0.166	0.168±0.108	0.050±0.029
FEXOFENADINE_MPO	0.971±0.006	0.521±0.032	0.573±0.022	0.510±0.026	0.562±0.008
GSK3B	0.965±0.030	0.314±0.148	0.141±0.023	0.134±0.045	0.163±0.040
ISOMERS_C7H8N2O2	0.990±0.000	0.760±0.068	0.078±0.099	0.045±0.067	0.055±0.087
ISOMERS_C9H10N2O2PF2CL	0.985±0.002	0.383±0.144	0.257±0.077	0.229±0.178	0.122±0.038
JNK3	0.429±0.039	0.091±0.048	0.075±0.022	0.083±0.023	0.072±0.034
MEDIAN1	0.388±0.005	0.097±0.030	0.139±0.013	0.141±0.025	0.146±0.039
MEDIAN2	0.386±0.026	0.166±0.014	0.154±0.013	0.154±0.007	0.155±0.009
MESTRANOL_SIMILARITY	0.990±0.000	0.285±0.030	0.275±0.030	0.303±0.025	0.284±0.014
OSIMERTINIB_MPO	0.827±0.046	0.708±0.014	0.670±0.037	0.654±0.078	0.636±0.073
PERINDOPRIL_MPO	0.791±0.005	0.344±0.023	0.354±0.018	0.364±0.029	0.352±0.019
QED	0.914±0.013	0.767±0.009	0.905±0.023	0.900±0.010	0.897±0.007
RANOLAZINE_MPO	0.824±0.011	0.401±0.187	0.297±0.128	0.238±0.037	0.215±0.066
SCAFFOLD_HOP	0.911±0.068	0.429±0.030	0.422±0.016	0.419±0.014	0.421±0.008
SITAGLIPTIN_MPO	0.204±0.046	0.129±0.065	0.095±0.041	0.131±0.052	0.168±0.045
THIOTHIXENE_REDISCOVERY	0.990±0.000	0.281±0.032	0.261±0.024	0.232±0.021	0.245±0.014
TROGLITAZONE_REDISCOVERY	0.962±0.025	0.214±0.031	0.197±0.014	0.202±0.020	0.206±0.027
VALSARTAN_SMARTS	0.121±0.119	0.000±0.000	0.000±0.000	0.000±0.000	0.000±0.000
ZALEPLON_MPO	0.684±0.038	0.351±0.057	0.364±0.042	0.269±0.046	0.339±0.065
SUM	19.852 ^{+0.409} _{-0.383}	8.501 ^{+0.829} _{-0.780}	7.064 ^{+0.512} _{-0.428}	7.041 ^{+0.486} _{-0.416}	6.949 ^{+0.341} _{-0.306}
RANK	1	2	3	4	5

Table D2. Top1 AUC over 10000 iterations. Performance comparison across molecular optimization tasks. Higher is better.

TASK	SEISMO	SEISMO _{No DESC.}	REINVENT	GRAPH GA	GP BO
ALBUTEROL_SIMILARITY	1.000±0.000	0.537±0.107	0.906±0.004	0.877±0.025	0.925±0.013
AMLODIPINE_MPO	0.905±0.001	0.532±0.032	0.655±0.042	0.688±0.023	0.609±0.049
CELECOXIB_REDISCOVERY	1.000±0.000	0.444±0.072	0.803±0.110	0.684±0.137	0.809±0.084
DECO_HOP	0.961±0.022	0.598±0.003	0.682±0.054	0.627±0.006	0.648±0.030
DRD2	1.000±0.000	0.673±0.558	0.968±0.008	0.991±0.002	0.958±0.008
FEXOFENADINE_MPO	0.992±0.008	0.611±0.048	0.804±0.008	0.777±0.013	0.743±0.008
GSK3B	0.983±0.029	0.482±0.123	0.894±0.050	0.829±0.078	0.879±0.044
ISOMERS_C7H8N2O2	1.000±0.000	0.860±0.128	0.884±0.033	0.899±0.067	0.747±0.125
ISOMERS_C9H10N2O2PF2CL	1.000±0.000	0.499±0.175	0.673±0.066	0.766±0.052	0.514±0.192
JNK3	0.503±0.075	0.163±0.097	0.814±0.028	0.598±0.159	0.593±0.179
MEDIAN1	0.400±0.000	0.135±0.024	0.368±0.011	0.320±0.031	0.317±0.019
MEDIAN2	0.395±0.028	0.193±0.021	0.290±0.010	0.289±0.009	0.310±0.011
MESTRANOL_SIMILARITY	1.000±0.000	0.378±0.033	0.639±0.054	0.617±0.031	0.667±0.092
OSIMERTINIB_MPO	0.938±0.044	0.791±0.026	0.852±0.012	0.849±0.007	0.806±0.006
PERINDOPRIL_MPO	0.810±0.000	0.431±0.024	0.555±0.019	0.561±0.012	0.514±0.015
QED	0.940±0.011	0.803±0.002	0.948±0.000	0.947±0.000	0.946±0.001
RANOLAZINE_MPO	0.939±0.004	0.558±0.185	0.789±0.011	0.760±0.015	0.763±0.015
SCAFFOLD_HOP	0.935±0.065	0.461±0.035	0.575±0.025	0.528±0.010	0.565±0.026
SITAGLIPTIN_MPO	0.294±0.043	0.219±0.108	0.055±0.017	0.492±0.076	0.238±0.069
THIOTHIXENE_REDISCOVERY	1.000±0.000	0.349±0.072	0.559±0.016	0.508±0.029	0.592±0.029
TROGLITAZONE_REDISCOVERY	1.000±0.000	0.311±0.019	0.460±0.038	0.411±0.019	0.432±0.018
VALSARTAN_SMARTS	0.230±0.205	0.000±0.000	0.187±0.418	0.000±0.000	0.000±0.000
ZALEPLON_MPO	0.729±0.024	0.418±0.080	0.383±0.070	0.367±0.038	0.252±0.079
SUM	21.173 ^{+0.586} _{-0.559}	10.443 ^{+0.911} _{-1.096}	14.741 ^{+0.946} _{-0.504}	14.383 ^{+0.447} _{-0.475}	13.832 ^{+0.598} _{-0.596}
RANK	1	5	2	3	4

Table D3. Best score after 50 iterations. Performance comparison across molecular optimization tasks. Higher is better.

TASK	SEISMO	SEISMO _{No DESC.}	REINVENT	GRAPH GA	GP BO
ALBUTEROL_SIMILARITY	1.000±0.000	0.538±0.108	0.390±0.028	0.422±0.034	0.412±0.039
AMLODIPINE_MPO	0.905±0.001	0.532±0.032	0.471±0.030	0.463±0.020	0.464±0.028
CELECOXIB_REDISCOVERY	1.000±0.000	0.444±0.073	0.297±0.046	0.293±0.033	0.285±0.033
DECO_HOP	0.961±0.022	0.598±0.003	0.572±0.012	0.818±0.008	0.820±0.011
DRD2	1.000±0.000	0.675±0.559	0.322±0.307	0.249±0.150	0.072±0.045
FEXOFENADINE_MPO	0.992±0.008	0.611±0.048	0.627±0.042	0.579±0.031	0.627±0.027
GSK3B	0.983±0.029	0.483±0.123	0.204±0.106	0.212±0.093	0.206±0.058
ISOMERS_C7H8N2O2	1.000±0.000	0.860±0.128	0.149±0.227	0.087±0.103	0.075±0.093
ISOMERS_C9H10N2O2PF2CL	1.000±0.000	0.500±0.175	0.411±0.077	0.422±0.162	0.354±0.181
JNK3	0.503±0.075	0.163±0.097	0.128±0.058	0.110±0.019	0.170±0.137
MEDIAN1	0.400±0.000	0.135±0.024	0.162±0.024	0.168±0.030	0.166±0.041
MEDIAN2	0.395±0.028	0.193±0.021	0.177±0.018	0.172±0.014	0.169±0.013
MESTRANOL_SIMILARITY	1.000±0.000	0.379±0.033	0.295±0.019	0.336±0.019	0.311±0.025
OSIMERTINIB_MPO	0.939±0.044	0.791±0.026	0.719±0.020	0.751±0.022	0.733±0.042
PERINDOPRIL_MPO	0.810±0.000	0.432±0.024	0.391±0.011	0.404±0.021	0.394±0.033
QED	0.940±0.010	0.803±0.002	0.924±0.019	0.924±0.015	0.932±0.006
RANOLAZINE_MPO	0.939±0.004	0.559±0.185	0.343±0.129	0.341±0.077	0.257±0.075
SCAFFOLD_HOP	0.935±0.065	0.461±0.035	0.438±0.014	0.439±0.014	0.433±0.011
SITAGLIPTIN_MPO	0.295±0.043	0.219±0.108	0.136±0.063	0.157±0.052	0.207±0.054
THIOTHIXENE_REDISCOVERY	1.000±0.000	0.350±0.073	0.279±0.026	0.258±0.037	0.282±0.031
TROGLITAZONE_REDISCOVERY	1.000±0.000	0.311±0.019	0.214±0.018	0.217±0.018	0.237±0.028
VALSARTAN_SMARTS	0.230±0.205	0.000±0.000	0.002±0.004	0.000±0.000	0.000±0.000
ZALEPLON_MPO	0.729±0.024	0.418±0.080	0.414±0.056	0.360±0.063	0.390±0.049
SUM	21.179 ^{+0.588} _{-0.561}	10.453 ^{+0.912} _{-1.098}	8.064 ^{+0.881} _{-0.618}	8.181 ^{+0.553} _{-0.481}	8.003 ^{+0.529} _{-0.480}
RANK	1	2	4	3	5

Table D4. Top10 AUC over 1000 iterations. Performance comparison across molecular optimization tasks. Higher is better.

TASK	SEISMO	SEISMO _{No Desc.}	GP BO	GRAPH GA	REINVENT	LICO	GENETIC GFN	AUGMENTED MEMORY	MOLLEO
ALBUTEROL_SIMILARITY	0.999 ± 0.000	0.495 ± 0.093	0.636 ± 0.106	0.583 ± 0.065	0.496 ± 0.020	0.656 ± 0.125	0.664 ± 0.054	0.557 ± 0.048	0.886 ± 0.023
AMLODIPINE_MPO	0.898 ± 0.001	0.516 ± 0.027	0.519 ± 0.014	0.501 ± 0.016	0.472 ± 0.008	0.541 ± 0.026	0.534 ± 0.019	0.489 ± 0.009	0.637 ± 0.023
CELECOXIB_REDISCOVERY	0.883 ± 0.002	0.422 ± 0.060	0.411 ± 0.046	0.424 ± 0.049	0.370 ± 0.029	0.447 ± 0.073	0.447 ± 0.028	0.385 ± 0.027	0.402 ± 0.003
DECO_HOP	0.956 ± 0.023	0.593 ± 0.003	0.593 ± 0.013	0.581 ± 0.006	0.572 ± 0.006	0.596 ± 0.010	0.604 ± 0.017	0.579 ± 0.010	0.588 ± 0.007
DRD2	0.999 ± 0.000	0.652 ± 0.541	0.857 ± 0.080	0.833 ± 0.065	0.775 ± 0.086	0.859 ± 0.066	0.809 ± 0.045	0.795 ± 0.024	0.910 ± 0.017
FEXOFENADINE_MPO	0.983 ± 0.003	0.595 ± 0.043	0.707 ± 0.021	0.666 ± 0.009	0.650 ± 0.007	0.700 ± 0.023	0.682 ± 0.021	0.679 ± 0.021	0.674 ± 0.002
GSK3B	0.974 ± 0.031	0.420 ± 0.130	0.611 ± 0.059	0.523 ± 0.047	0.589 ± 0.063	0.617 ± 0.063	0.637 ± 0.018	0.539 ± 0.097	0.397 ± 0.013
ISOMERS_C7H8N2O2	0.999 ± 0.001	0.796 ± 0.112	0.545 ± 0.158	0.735 ± 0.112	0.725 ± 0.064	0.779 ± 0.099	0.738 ± 0.039	0.661 ± 0.039	0.737 ± 0.043
ISOMERS_C9H10N2O2PF2CL	0.998 ± 0.000	0.443 ± 0.147	0.599 ± 0.059	0.630 ± 0.086	0.630 ± 0.032	0.672 ± 0.075	0.656 ± 0.075	0.596 ± 0.066	0.635 ± 0.017
JNK3	0.464 ± 0.065	0.134 ± 0.077	0.346 ± 0.067	0.301 ± 0.071	0.315 ± 0.042	0.336 ± 0.051	0.409 ± 0.165	0.294 ± 0.110	0.186 ± 0.076
MEDIAN1	0.343 ± 0.001	0.129 ± 0.023	0.213 ± 0.020	0.208 ± 0.015	0.205 ± 0.012	0.217 ± 0.019	0.219 ± 0.008	0.219 ± 0.014	0.236 ± 0.021
MEDIAN2	0.365 ± 0.028	0.183 ± 0.018	0.203 ± 0.009	0.181 ± 0.009	0.188 ± 0.010	0.193 ± 0.009	0.204 ± 0.011	0.184 ± 0.010	0.191 ± 0.009
MESTRANOL_SIMILARITY	0.999 ± 0.000	0.353 ± 0.032	0.427 ± 0.025	0.362 ± 0.017	0.379 ± 0.026	0.423 ± 0.016	0.414 ± 0.022	0.393 ± 0.021	0.399 ± 0.020
OSIMERTINIB_MPO	0.924 ± 0.047	0.775 ± 0.024	0.766 ± 0.006	0.751 ± 0.005	0.737 ± 0.007	0.759 ± 0.008	0.763 ± 0.008	0.761 ± 0.006	0.779 ± 0.006
PERINDOPRIL_MPO	0.809 ± 0.000	0.419 ± 0.028	0.458 ± 0.019	0.435 ± 0.016	0.404 ± 0.009	0.473 ± 0.009	0.462 ± 0.033	0.422 ± 0.013	0.655 ± 0.054
QED	0.937 ± 0.010	0.799 ± 0.001	0.912 ± 0.010	0.914 ± 0.007	0.921 ± 0.002	0.925 ± 0.005	0.928 ± 0.002	0.923 ± 0.002	0.919 ± 0.006
RANOLAZINE_MPO	0.926 ± 0.004	0.536 ± 0.191	0.701 ± 0.023	0.620 ± 0.014	0.574 ± 0.044	0.687 ± 0.029	0.623 ± 0.022	0.614 ± 0.033	0.640 ± 0.000
SCAFFOLD_HOP	0.931 ± 0.065	0.457 ± 0.035	0.478 ± 0.009	0.461 ± 0.008	0.447 ± 0.010	0.480 ± 0.008	0.485 ± 0.015	0.460 ± 0.010	0.473 ± 0.000
SITAGLIPTIN_MPO	0.234 ± 0.059	0.173 ± 0.085	0.232 ± 0.083	0.229 ± 0.053	0.261 ± 0.026	0.315 ± 0.097	0.227 ± 0.041	0.245 ± 0.030	0.193 ± 0.073
THIOTHIXENE_REDISCOVERY	0.919 ± 0.041	0.333 ± 0.067	0.351 ± 0.039	0.322 ± 0.023	0.311 ± 0.021	0.343 ± 0.035	0.377 ± 0.015	0.336 ± 0.033	0.416 ± 0.075
TROGLITAZONE_REDISCOVERY	0.813 ± 0.083	0.287 ± 0.026	0.313 ± 0.018	0.267 ± 0.015	0.246 ± 0.009	0.292 ± 0.028	0.277 ± 0.015	0.262 ± 0.012	0.302 ± 0.022
VALSARTAN_SMARTS	0.137 ± 0.119	0.000 ± 0.000	0.000 ± 0.000	0.000 ± 0.000	0.000 ± 0.000	0.000 ± 0.000	0.000 ± 0.000	0.000 ± 0.000	0.000 ± 0.000
ZALEPLON_MPO	0.666 ± 0.034	0.398 ± 0.072	0.392 ± 0.034	0.374 ± 0.024	0.406 ± 0.017	0.404 ± 0.022	0.400 ± 0.014	0.415 ± 0.013	0.392 ± 0.003
SUM OF SCORES (†)	20.24	9.91	11.27	10.90	10.68	11.71	11.56	10.81	11.65

E. Example prompts, explanations and optimization trajectory

E.1. System prompt defining the LLM-guided molecular optimization protocol

The prompt below specifies a closed-loop proposal mechanism in which the language model is conditioned on the complete history of previously evaluated molecules and is required to output exactly one new candidate per iteration in a fixed JSON format.

You are an expert medicinal chemist whose job is to propose and optimize new molecules.

You interact in a multi-step optimization loop.

In this loop you:

- Propose small organic molecules as SMILES strings.
- Receive evaluations of your proposals.
- Have access to the full conversation history, including all past proposals, rationales, and evaluations.

Your goal in this conversation is to iteratively propose new molecules that move the objective toward the specified target, using the information in the conversation history and your general chemical knowledge.

OUTPUT FORMAT:

For every proposal, you must respond with a single JSON object of the form

```
{
  "reason": "<short explanation>",
  "smiles": "<SMILES string>"
}
```

Requirements:

- "smiles" must be a single, valid SMILES string for a plausible small molecule.
- "reason" should briefly explain why, given the history of molecules and their scores, this new proposal might improve or further explore the objective landscape.
- Do not repeat any previous molecule exactly. The scores are deterministic and will not change if a molecule is re-evaluated.
- Do not include any text outside the JSON object. No Markdown, no comments, no code fences.

E.2. PMO benchmark first messages

For the PMO benchmark, we include three example first messages—Celecoxib rediscovery, Osimertinib MPO and DRD2—to illustrate the prompting setup. These messages follow the level of explicitness established in prior literature such as MolLEO and LICO. For brevity, the remaining 20 first messages for the other tasks are available in the project’s GitHub repository.

Rediscovery task: The rediscovery score ($[0,1]$, higher is better) measures the Tanimoto
 \rightarrow similarity with the SMILES of celecoxib.

Objective:

- maximize the similarity score (0-1; higher is better).
- You will have 50 iterations to optimize the molecule.

Step 1:

Propose a single initial molecule as a SMILES string that you think will achieve a high
 \rightarrow similarity score to celecoxib.

Respond with a single JSON object: {"reason": "<why this is a reasonable starting point
 \rightarrow for this objective>", "smiles": "<SMILES string>"}

Osimertinib MPO: score is the geometric mean of 4 terms (each in $[0,1]$):

score = gmean([sim_v1, sim_v2, tpsa_term, logp_term])

Reference molecule (Osimertinib) SMILES:

COc1cc(N(C)CCN(C)C)c(NC(=O)C=C)cc1Nc2nccc(n2)c3cn(C)c4cccc34

Terms:

sim_v1 = clip(Tanimoto(FCFP4(test), FCFP4(ref)), t=0.8)

sim_v2 = min_gauss(Tanimoto(ECFP6(test), ECFP6(ref)); mu=0.85, sigma=0.1)

tpsa_term = max_gauss(TPSA(test); mu=100, sigma=10)

logp_term = min_gauss(MolLogP(test); mu=1, sigma=1)

Modifiers:

clip(x,t) = 1 if $x \geq t$ else x/t

min_gauss(x;mu,s) = 1 if $x \leq \mu$ else $\exp(-0.5 * ((x-\mu)/s)^2)$

max_gauss(x;mu,s) = 1 if $x \geq \mu$ else $\exp(-0.5 * ((x-\mu)/s)^2)$

Objective:

- maximize the Osimertinib MPO score (0-1; higher is better).
- You will have 50 iterations to optimize the molecule.

Step 1:

Propose a single initial molecule as a SMILES string that you think will have a high MPO
 \rightarrow score by:

- being similar to Osimertinib under BOTH similarity terms (FCFP4 similarity clipped at
 \rightarrow 0.8, and ECFP6 similarity favored up to ~ 0.85),
- having TPSA in the high-preferred region (max-Gaussian with target around 100), and
- having logP in the low-preferred region (min-Gaussian with target around 1).

Respond with a single JSON object: {"reason": "<why this is a reasonable starting point for
 \rightarrow this objective>", "smiles": "<SMILES string>"}

Optimize predicted bioactivity against Dopamine Receptor D2 (DRD2). Scores are in $[0, 1]$
 \rightarrow with higher being better.

Objective:

- maximize the predicted DRD2 activity score (0-1; higher is better).
- You will have 50 iterations to optimize the molecule.

Step 1:

Propose a single initial molecule as a SMILES string that you think has good predicted
 \rightarrow bioactivity against DRD2.

Respond with a single JSON object: {"reason": "<why this is a reasonable starting point for
 \rightarrow this objective>", "smiles": "<SMILES string>"}

SEISMO: Increasing Sample Efficiency in Molecular Optimization with a Trajectory-Aware LLM Agent

```
| -0.101324 | 0 | 104 | [!#6;!#1;!H0]~*~[CH2]~* |  
| -0.115687 | 1 | 48 | [#8]~[!#6;!#1] (~[#8]) (~[#8]) |
```

Similarity explanation using O=C1c3c(O/C(=C1/O)c2ccc(O)c(O)c2)cc(O)cc3O (Quercetin) as Target molecule and O=C1c2c(OC)cc(O)cc2OC(=C1OC)c3ccc(OC)cc3 as Query molecule, which was generated by the agent:

The following 3 features are present in TARGET but not in QUERY (reducing similarity):

Key 53: [!#6;!#1;!H0]~*~*~*~[!#6;!#1;!H0]

Key 54: [!#6;!#1;!H0]~*~*~[!#6;!#1;!H0]

Key 131: [!#6;!#1;!H0] (count > 1)

The following 5 features are present in QUERY but not in TARGET (reducing similarity):

Key 93: [!#6;!#1]~[CH3]

Key 126: *!@[#8]!@*

Key 141: [CH3] (count > 2)

Key 149: [C;H3,H4] (count > 1)

Key 160: [C;H3,H4]

Boltz-2 explanation using the SARS-CoV-2 M^{PRO} sequence as target:

Close Residues (within 5.0 Å):

THR-26, THR-27, LEU-28, HIS-42, CYS-45, THR-46, SER-47, MET-50, PHE-141, LEU-142, ASN-143,
↪ GLY-144, SER-145, CYS-146, HIS-164, HIS-165, MET-166, GLU-167, HIS-173, VAL-187,
↪ ASP-188, ARG-189, GLN-190, GLN-193

Confidence Scores:

confidence_score: 0.9855

ptm: 0.9857

iptm: 0.9813

ligand_iptm: 0.9813

complex_plddt: 0.9865

complex_iplddt: 0.9793

complex_pde: 0.2956

complex_ipde: 0.4609

E.4. Example optimization trajectory showing the generated JSON (containing SMILES and rationale) for each iteration

The conversation below was generated using the Claude Opus 4.5 model. The goal was to reduce the XGBoost-predicted IC₅₀ to below 1 nM while achieving a QED of at least 0.6 and ensuring the final molecule is novel (not listed in PubChem). Because these thresholds were highly ambitious, the generative agent did not meet all objectives and ran for the maximum of 50 iterations. The “full explanation” mode was enabled, providing QED and IC₅₀ oracle explanations at each iteration like shown in Appendix E.3 for iteration 4. The rest is available on our GitHub. When an iteration is missing, the parsing or validity checks failed.

Iteration 1: "reason": "Starting with a peptidomimetic scaffold commonly found in protease inhibitors. This molecule features a hydroxyl group for transition state mimicry, aromatic groups for S1/S2 pocket binding, and an amide backbone typical of protease substrates. The structure is based on successful HIV protease inhibitor scaffolds but modified to be potentially novel while maintaining drug-like properties.", "smiles": "CC(C)CC(NC(=O)C(Cc1cccc1)NC(=O)OC)C(O)Cc1cccc1""

Scores: "IC50": 94377.57, "QED": 0.560, "Novelty": Yes

Iteration 2: "reason": "The previous molecule had too many rotatable bonds, high MW, and multiple HBD hurting QED. SHAP analysis shows adding sulfur, halogens, and C=O groups could improve IC50. I'm designing a more rigid, smaller molecule with a sulfonamide group, fluorine substituent, and fewer rotatable bonds while maintaining key pharmacophoric features for protease inhibition.", "smiles": "Fc1ccc(S(=O)(=O)Nc2ccc(C(=O)NC3CCCC3)cc2)cc1""

Scores: "IC50": 810.56, "QED": 0.836, "Novelty": No

Iteration 3: "reason": "The previous molecule improved IC50 significantly but exists in PubChem. SHAP shows positive contributions from sulfur, multiple C=O groups, and ring nitrogen. I'll modify the structure by adding a nitrogen-containing heterocycle (pyridine), keeping the sulfonamide, and adding a trifluoromethyl group for novelty while maintaining the beneficial features. The cyclopentyl instead of cyclohexyl adds novelty.", "smiles": "FC(F)(F)c1ccc(S(=O)(=O)Nc2ccc(C(=O)NC3CCCC3)nc2)cc1""

Scores: "IC50": 2907.69, "QED": 0.784, "Novelty": Yes

Iteration 4: "reason": "SHAP analysis shows sulfur (key 88) absence hurts IC50, and multiple 6-membered rings (key 145) would help. Adding back sulfur via sulfonamide, including a 6-membered heterocyclic ring with nitrogen (key 121 positive), and keeping halogens. I'll design a molecule with a thiazole ring system, sulfonamide, and fluorine to maximize positive SHAP contributions while ensuring novelty.", "smiles": "Fc1ccc(S(=O)(=O)Nc2nc3cccc3s2)cc1C(=O)NC1CCCC1""

Scores: "IC50": 491.44, "QED": 0.628, "Novelty": Yes

Iteration 5: "reason": "IC50 improved to 491 nM. SHAP shows multiple 6-membered rings (key 145) and sulfur (key 88) help significantly. QED is hurt by 3 aromatic rings and high MW. I'll reduce to 2 aromatic rings, keep sulfur via thioether instead of sulfonamide, add N~*~*~*~N pattern (key 80), and include a smaller cyclic amine to reduce MW while maintaining beneficial features.", "smiles": "Fc1ccc(Sc2ccc(C(=O)N3CCNCC3)nc2)cc1""

Scores: "IC50": 8718.88, "QED": 0.944, "Novelty": Yes

Iteration 6: "reason": "SHAP analysis shows key 137 ([!C;!c;R] - heteroatom in ring) and key 136 (multiple C=O) have strong negative impact when absent. Key 145 (multiple 6-membered rings) and key 134 (halogens) also help. I'll design a molecule with a saturated heterocyclic ring containing heteroatom, multiple carbonyl groups, multiple 6-membered rings, and halogen while keeping sulfur and good QED properties.", "smiles": "Fc1ccc(S(=O)(=O)N2CCN(C(=O)c3ccnc3)CC2)cc1""

Scores: "IC50": 12561.47, "QED": 0.839, "Novelty": No

Iteration 7: "reason": "Looking at best performer (491 nM), key features were: multiple
 ↪ 6-membered rings (key 145), sulfur (key 88), heteroatom in ring (key 137), multiple
 ↪ C=O (key 136), and halogen (key 134). The molecule also had benzothiazole. I'll create
 ↪ a novel variant with benzothiazole core, add a second 6-membered ring, include
 ↪ multiple carbonyls, keep fluorine, and add a hydroxyl group for key 104
 ↪ ([!#6;!#1;!H0]~*~[CH2]~*) contribution.", "smiles":
 ↪ "Fc1ccc2nc(NC(=O)c3ccc(C(=O)NC4CCOCC4)cc3)sc2c1"

Scores: "IC50": 2449.49, "QED": 0.703, "Novelty": Yes

Iteration 8: "reason": "Key 145 (multiple 6-membered rings) has strong negative impact
 ↪ when absent (-0.171). Best molecule had pIC50=6.31 with benzothiazole. I need to add
 ↪ multiple 6-membered rings, keep sulfur, add key 92 (O~C(~N)~C pattern via amide), key
 ↪ 104 ([!#6;!#1;!H0]~*~[CH2]~*), and reduce aromatic rings to 2 for QED. Using
 ↪ cyclohexyl with hydroxyl group attached to CH2.", "smiles":
 ↪ "Fc1ccc2sc(NC(=O)c3cccc(F)c3)nc2c1CC(O)C1CCCCC1"

Scores: "IC50": 1021.78, "QED": 0.592, "Novelty": Yes

Iteration 9: "reason": "IC50 improved to 1022 nM but QED failed due to high ALOGP (5.31)
 ↪ and 3 aromatic rings. Key 145 (multiple 6-membered rings) gave +0.31 boost. Key 137
 ↪ (heteroatom in ring) absence hurt (-0.17). I'll keep multiple 6-membered rings but
 ↪ reduce lipophilicity by using morpholine instead of cyclohexyl, reduce to 2 aromatic
 ↪ rings, and add heteroatom in ring to satisfy key 137.", "smiles":
 ↪ "Fc1ccc2sc(NC(=O)c3ccncc3)nc2c1CN1CCOCC1"

Scores: "IC50": 1061.66, "QED": 0.763, "Novelty": Yes

Iteration 10: "reason": "Key 137 (heteroatom in ring) absence still hurts (-0.17). Key 104
 ↪ ([!#6;!#1;!H0]~*~[CH2]~*) absence also hurts (-0.12). QED penalized by 3 aromatic
 ↪ rings. I'll use a piperidine ring (satisfies key 137), add NH adjacent to CH2 (key
 ↪ 104), reduce to 2 aromatic rings by replacing pyridine with saturated ring, and keep
 ↪ beneficial features: multiple 6-membered rings, sulfur, halogen, carbonyl.", "smiles":
 ↪ "Fc1ccc(S(=O)(=O)NC2CCN(C(=O)c3ccccc3)CC2)cc1"

Scores: "IC50": 5591.23, "QED": 0.908, "Novelty": No

Iteration 11: "reason": "Best IC50 was 491 nM with benzothiazole scaffold. Key features
 ↪ needed: multiple 6-membered rings (key 145, +0.30), heteroatom in ring (key 137),
 ↪ multiple C=O (key 136), halogen (key 134), sulfur (key 88). Key 81 (S with 3
 ↪ connections) hurts, so avoid sulfonamide. I'll use benzothiazole with simple thioether
 ↪ sulfur, add a second 6-membered ring via cyclohexyl amide, include fluorine, and add a
 ↪ methyl group for novelty.", "smiles": "Cc1ccc2nc(NC(=O)C3CCCC3)sc2c1F"

Scores: "IC50": 752.34, "QED": 0.898, "Novelty": Yes

Iteration 12: "reason": "Good progress at 752 nM with excellent QED. Key 137 (heteroatom
 ↪ in ring) absence still hurts (-0.17). Key 104 ([!#6;!#1;!H0]~*~[CH2]~*) absence hurts
 ↪ (-0.09). I'll add a piperidine ring to satisfy key 137 and key 104 (NH adjacent to
 ↪ CH2), while keeping the beneficial benzothiazole core, multiple 6-membered rings,
 ↪ fluorine, and sulfur. This should push IC50 lower.", "smiles":
 ↪ "Cc1ccc2nc(NC(=O)C3CCNCC3)sc2c1F"

Scores: "IC50": 2377.80, "QED": 0.895, "Novelty": Yes

Iteration 13: "reason": "The piperidine NH hurt IC50 (key 84 NH2 negative). Best was 752
 ↪ nM with cyclohexyl. Key 137 (heteroatom in saturated ring) absence hurts most (-0.21).
 ↪ I need a saturated ring with heteroatom but NOT NH. I'll use morpholine (O in ring
 ↪ satisfies key 137) attached via N-acyl, keeping benzothiazole, fluorine, and methyl.
 ↪ This avoids the NH penalty while adding the heteroatom in ring.", "smiles":
 ↪ "Cc1ccc2nc(NC(=O)CN3CCOCC3)sc2c1F"

Scores: "IC50": 839.39, "QED": 0.942, "Novelty": Yes

SEISMO: Increasing Sample Efficiency in Molecular Optimization with a Trajectory-Aware LLM Agent

Iteration 14: "reason": "Key 137 (heteroatom in saturated ring) absence still hurts most
→ (-0.18). Key 104 ([!#6;!#1;!H0]~*~[CH2]~*) absence also hurts (-0.15). The morpholine
→ oxygen doesn't satisfy key 137 which requires [!C;!c;R] - a non-carbon in a ring. I
→ need a nitrogen IN the ring that's not NH. I'll use N-methylpiperazine which has ring
→ nitrogen (satisfies key 137) and also provides key 104 pattern. Keep benzothiazole
→ core with fluorine.", "smiles": "Cc1ccc2nc(NC(=O)CN3CCN(C)CC3)sc2c1F"

Scores: "IC50": 1352.25, "QED": 0.938, "Novelty": Yes

Iteration 15: "reason": "Key 137 still absent and hurting (-0.18). The piperazine
→ nitrogens are tertiary (no H), so they don't count as [!C;!c;R]. Key 104
→ ([!#6;!#1;!H0]~*~[CH2]~*) needs heteroatom with H adjacent to CH2. Best IC50 was 752
→ nM with cyclohexyl amide. I'll go back to that scaffold but add a hydroxyl group on
→ the cyclohexyl to satisfy key 104 (OH~CH2) and potentially key 137 if I use a
→ saturated heterocycle with NH instead.", "smiles":
→ "Cc1ccc2nc(NC(=O)C3CC(O)CCC3)sc2c1F"

Scores: "IC50": 744.23, "QED": 0.895, "Novelty": Yes

Iteration 16: "reason": "IC50 at 744 nM is good. Key 140 (>3 oxygens) hurts significantly
→ (-0.26). Key 137 (heteroatom in ring) absence hurts (-0.16). Key 104 absence hurts
→ (-0.08). I'll remove the hydroxyl to avoid key 140 penalty, and instead use a
→ piperidinone ring which has both N in ring (key 137) and C=O (key 136). This should
→ satisfy key 137 without adding extra oxygens.", "smiles":
→ "Cc1ccc2nc(NC(=O)C3CCC(=O)NC3)sc2c1F"

Scores: "IC50": 320.67, "QED": 0.893, "Novelty": Yes

Iteration 17: "reason": "Excellent progress! IC50 dropped to 321 nM with piperidinone. Key
→ 137 now contributes +0.16. Key 156 (N with 3 connections) absence hurts (-0.11). Key
→ 104 absence still hurts (-0.09). Key 80 (N~*~*~*~N) absence hurts (-0.06). I'll add a
→ tertiary nitrogen to satisfy key 156, and extend the chain to create N~*~*~*~N pattern
→ (key 80). Adding N-methyl to the lactam should help.", "smiles":
→ "Cc1ccc2nc(NC(=O)C3CCC(=O)N(C)C3)sc2c1F"

Scores: "IC50": 169.35, "QED": 0.924, "Novelty": Yes

Iteration 18: "reason": "Great progress at 169 nM! Key 104 ([!#6;!#1;!H0]~*~[CH2]~*)
→ absence hurts most (-0.14). Key 156 (N with 3 connections) absence hurts (-0.12). Key
→ 80 (N~*~*~*~N) absence hurts (-0.07). I'll add a hydroxyl group on the piperidinone
→ ring to satisfy key 104 (OH adjacent to CH2), and this should also help with key 43.
→ The N-methyl lactam worked well, keeping that.", "smiles":
→ "Cc1ccc2nc(NC(=O)C3CC(O)C(=O)N(C)C3)sc2c1F"

Scores: "IC50": 2055.81, "QED": 0.870, "Novelty": Yes

Iteration 19: "reason": "Adding hydroxyl hurt IC50 badly due to key 140 (>3 oxygens,
→ -0.32). Going back to the 169 nM scaffold without extra oxygen. Key 104 absence hurts
→ (-0.14) but adding OH causes worse penalty. Key 156 (N~*(~*)~*) absence hurts (-0.12).
→ I'll try adding a second nitrogen in the ring system to create N~*~*~*~N pattern (key
→ 80) and potentially satisfy key 156 by using a piperazinone instead of piperidinone.",
→ "smiles": "Cc1ccc2nc(NC(=O)C3CN(C)C(=O)CN3C)sc2c1F"

Scores: "IC50": 241.84, "QED": 0.902, "Novelty": Yes

Iteration 20: "reason": "The N-methyl piperidinone (169 nM) was better than the
→ diketopiperazine (242 nM). Key 104 absence still hurts (-0.14). Key 129 (CH2~*~*~CH2
→ pattern) absence hurts (-0.12). I'll go back to the N-methyl piperidinone scaffold and
→ try to add key 129 by extending with a CH2 chain, and add key 156 (tertiary N) by
→ including a dimethylamino group on the benzothiazole.", "smiles":
→ "CN(C)c1ccc2nc(NC(=O)C3CCC(=O)N(C)C3)sc2c1"

Scores: "IC50": 44128.01, "QED": 0.935, "Novelty": Yes

Iteration 21: "reason": "The dimethylamino substitution destroyed IC50 - key 145 (multiple
↪ 6-membered rings) and key 108 now absent and hurting badly. Going back to the best
↪ scaffold (169 nM) with fluorine and methyl on benzothiazole. Key 104 absence still
↪ hurts. I'll try adding a chlorine instead of fluorine (stronger halogen effect) and
↪ slightly modify the lactam ring to a 5-membered pyrrolidinone to see if that helps
↪ while maintaining key features.", "smiles": "Cc1ccc2nc(NC(=O)C3CCC(=O)N3C)sc2c1C1"

Scores: "IC50": 157.35, "QED": 0.924, "Novelty": Yes

Iteration 22: "reason": "Excellent! 157 nM with 5-membered pyrrolidinone and chlorine. Key
↪ 104 now contributes +0.31! Key 129 (CH2~*~*~CH2 pattern) absence hurts (-0.16). Key
↪ 130 ([!#6;!#1]~[!#6;!#1] count>1) absence hurts (-0.09). I'll try to add key 129 by
↪ using a 6-membered piperidinone instead (has CH2~*~*~CH2 pattern), keep chlorine and
↪ the beneficial scaffold. Also try adding a second halogen for key 130.", "smiles":
↪ "Cc1ccc2nc(NC(=O)C3CCC(=O)N(C)C3)sc2c1C1"

Scores: "IC50": 116.91, "QED": 0.916, "Novelty": Yes

Iteration 23: "reason": "Great progress at 117 nM! Key 156 (N~*(~*)~*) absence hurts
↪ (-0.11). Key 80 (N~*~*~*~N) absence hurts (-0.10). Key 48 presence hurts (-0.11). I'll
↪ try to add key 156 by making the lactam nitrogen more substituted, and add key 80 by
↪ including a second nitrogen in the system. Using a piperazinone ring instead of
↪ piperidinone should provide both N~*~*~*~N pattern and tertiary nitrogen.", "smiles":
↪ "Cc1ccc2nc(NC(=O)C3CCN(C)C(=O)N3C)sc2c1C1"

Scores: "IC50": 108.01, "QED": 0.903, "Novelty": Yes

Iteration 24: "reason": "108 nM is good progress. Key 129 (CH2~*~*~CH2 pattern) absence
↪ hurts most (-0.17). Key 156 (N~*(~*)~*) absence hurts (-0.11). Key 130 absence hurts
↪ (-0.09). I'll try a 7-membered ring lactam which would have the CH2~*~*~CH2 pattern
↪ (key 129), keep the chlorine and benzothiazole scaffold. This should satisfy key 129
↪ while maintaining other beneficial features.", "smiles":
↪ "Cc1ccc2nc(NC(=O)C3CCCC(=O)N(C)C3)sc2c1C1"

Scores: "IC50": 182.31, "QED": 0.901, "Novelty": Yes

Iteration 25: "reason": "The 7-membered ring (182 nM) was worse than 6-membered (117 nM).
↪ Going back to the best scaffold. Key 156 (N~*(~*)~*) absence hurts (-0.11). Key 80
↪ (N~*~*~*~N) absence hurts (-0.10). I'll try adding a tertiary amine substituent on the
↪ benzothiazole ring via a methylene linker to satisfy key 156 while keeping the
↪ successful piperidinone core with chlorine.", "smiles":
↪ "Cc1cc(CN(C)C)c2nc(NC(=O)C3CCC(=O)N(C)C3)sc2c1C1"

Scores: "IC50": 80.30, "QED": 0.865, "Novelty": Yes

Iteration 26: "reason": "80 nM is great progress! Key 80 (N~*~*~*~N) absence still hurts
↪ (-0.10). Key 48 presence hurts (-0.12). Key 94 presence hurts (-0.12). The
↪ dimethylamino helped but added penalties. I'll try a simpler modification - adding a
↪ second chlorine to the benzothiazole to increase halogen contribution (key 134) and
↪ potentially satisfy key 130 ([!#6;!#1]~[!#6;!#1] count>1), while keeping the
↪ successful piperidinone core.", "smiles": "Clc1cc(Cl)c2nc(NC(=O)C3CCC(=O)N(C)C3)sc2c1"

Scores: "IC50": 937.08, "QED": 0.895, "Novelty": Yes

Iteration 27: "reason": "Removing the methyl group destroyed key 145 (multiple 6-membered
↪ rings, -0.20). Going back to the 80 nM scaffold with methyl, chlorine, and
↪ dimethylaminomethyl. Key 80 (N~*~*~*~N) absence hurts (-0.10). I'll try to create this
↪ pattern by adding a nitrogen in the lactam ring system. Using a piperazinone instead
↪ of piperidinone should give N~*~*~*~N pattern while keeping other beneficial
↪ features.", "smiles": "Cc1cc(CN(C)C)c2nc(NC(=O)C3CN(C)C(=O)CC3)sc2c1C1"

Scores: "IC50": 80.30, "QED": 0.865, "Novelty": Yes

SEISMO: Increasing Sample Efficiency in Molecular Optimization with a Trajectory-Aware LLM Agent

Iteration 28: "reason": "Same 80 nM result. Key 80 (N~*~*~*~N) absence hurts (-0.10). Key
→ 48 presence hurts (-0.12). Key 94 presence hurts (-0.12). I'll try removing the
→ dimethylamino group (reduces key 94 penalty) and instead add a fluorine to create key
→ 80 pattern differently. Using the simpler scaffold with both Cl and F on
→ benzothiazole, keeping the successful piperidinone.", "smiles":
→ "Fclcc(C)c2nc(NC(=O)C3CCC(=O)N(C)C3)sc2c1Cl"

Scores: "IC50": 61.52, "QED": 0.899, "Novelty": Yes

Iteration 29: "reason": "Excellent progress at 61.5 nM! Key 43
→ ([!#6;!#1;!H0]~*~[!#6;!#1;!H0]) now contributes +0.16 with F and Cl adjacent. Key 156
→ (N~*(~*)~*) absence still hurts (-0.12). Key 80 (N~*~*~*~N) absence hurts (-0.10).
→ I'll try adding a small substituent that creates a tertiary nitrogen pattern. Adding
→ an N-ethyl instead of N-methyl on the lactam might help with key 156.", "smiles":
→ "Fclcc(C)c2nc(NC(=O)C3CCC(=O)N(CC)C3)sc2c1Cl"

Scores: "IC50": 17.80, "QED": 0.899, "Novelty": Yes

Iteration 30: "reason": "Excellent progress at 17.8 nM! N-ethyl instead of N-methyl helped
→ significantly. Key 115 (CH3~*~CH2~*) now contributes +0.19. Key 80 (N~*~*~*~N) absence
→ still hurts (-0.10). Key 48 presence hurts (-0.12). I'll try extending to N-propyl to
→ further enhance key 115 and potentially add key 129 (CH2~*~*~CH2 pattern), while
→ keeping the successful scaffold.", "smiles":
→ "Fclcc(C)c2nc(NC(=O)C3CCC(=O)N(CCC)C3)sc2c1Cl"

Scores: "IC50": 48.02, "QED": 0.868, "Novelty": Yes

Iteration 31: "reason": "N-propyl (48 nM) was worse than N-ethyl (17.8 nM). Key 117
→ (N~*~O) absence now hurts (-0.09). Going back to N-ethyl scaffold. Key 80 (N~*~*~*~N)
→ absence still hurts (-0.10). I'll try adding a small nitrogen-containing group to
→ create the N~*~*~*~N pattern. Adding an aminomethyl group on the benzothiazole should
→ create this pattern while keeping the successful core.", "smiles":
→ "Fclcc(CN)c2nc(NC(=O)C3CCC(=O)N(CC)C3)sc2c1Cl"

Scores: "IC50": 13.66, "QED": 0.848, "Novelty": Yes

Iteration 32: "reason": "13.7 nM is great! Key 80 (N~*~*~*~N) absence still hurts (-0.10).
→ Key 150 (*!@*~*!@*) absence now hurts (-0.03). The aminomethyl helped. I'll try
→ methylating the amine to reduce key 84 (NH2) penalty while potentially creating key 80
→ pattern. Using dimethylaminomethyl instead of aminomethyl.", "smiles":
→ "Fclcc(CN(C)C)c2nc(NC(=O)C3CCC(=O)N(CC)C3)sc2c1Cl"

Scores: "IC50": 23.30, "QED": 0.817, "Novelty": Yes

Iteration 33: "reason": "Dimethylamino (23 nM) was worse than primary amine (13.7 nM). Key
→ 94 ([!#6;!#1]~[#7]) presence hurts (-0.12). Going back to aminomethyl version. Key 80
→ (N~*~*~*~N) absence still hurts (-0.10). I'll try a different approach - adding a
→ cyano group instead which might satisfy key 80 pattern differently and avoid the amine
→ penalties. Or try isopropyl instead of ethyl on the lactam.", "smiles":
→ "Fclcc(C)c2nc(NC(=O)C3CCC(=O)N(C(C)C)C3)sc2c1Cl"

Scores: "IC50": 29.26, "QED": 0.871, "Novelty": Yes

Iteration 34: "reason": "Isopropyl (29 nM) was worse than ethyl (17.8 nM). Best so far is
→ aminomethyl with N-ethyl (13.7 nM). Key 156 (N~*(~*)~*) absence hurts (-0.15). Key 80
→ (N~*~*~*~N) absence hurts (-0.08). I'll try combining the aminomethyl group with
→ N-ethyl lactam, and add a methyl group on the amine to create a secondary amine
→ (methylaminomethyl) which might reduce NH2 penalty while keeping some benefit.",
→ "smiles": "Fclcc(CNC)c2nc(NC(=O)C3CCC(=O)N(CC)C3)sc2c1Cl"

Scores: "IC50": 9.36, "QED": 0.811, "Novelty": Yes

Iteration 42: "reason": "Removing the amine (8.73 nM) was worse than keeping it (2.47 nM).
 ↪ Key 83 ([!#6;!#1]1~*~*~*~1) absence now hurts (-0.05). The methylaminomethyl group
 ↪ was important. Going back to best scaffold (2.47 nM). Key 48 hurts (-0.11). I'll try
 ↪ replacing the secondary amine with an ether linkage (OCH3 instead of NHCH3) to reduce
 ↪ key 94 penalty while keeping similar size.", "smiles":
 ↪ "Fc1cc(COC)c2nc(NC(=O)C3CCCN(CC)C(=O)N3C)sc2c1C1"

Scores: "IC50": 6.33, "QED": 0.787, "Novelty": Yes

Iteration 43: "reason": "Methoxy (6.33 nM) was worse than methylamino (2.47 nM). The amine
 ↪ contributes positively despite key 94 penalty. Key 83 ([!#6;!#1]1~*~*~*~1) absence
 ↪ hurts (-0.06). Going back to best scaffold. I'll try adding a 5-membered heterocyclic
 ↪ ring to satisfy key 83 while keeping the methylaminomethyl. Using a pyrrolidine ring
 ↪ attached to the benzothiazole.", "smiles":
 ↪ "Fc1cc2nc(NC(=O)C3CCCN(CC)C(=O)N3C)sc2cc1C1"

Scores: "IC50": 12.26, "QED": 0.879, "Novelty": Yes

Iteration 45: "reason": "Invalid SMILES in last attempt. Going back to the best scaffold
 ↪ (2.47 nM). Key 48 presence hurts (-0.11). Key 94 presence hurts (-0.10). I'll try a
 ↪ different approach - using a cyclopropylmethyl group instead of ethyl on the
 ↪ diazepanone nitrogen, which might reduce some penalties while maintaining the
 ↪ beneficial features.", "smiles": "Fc1cc(CNC)c2nc(NC(=O)C3CCCN(CC4CC4)C(=O)N3C)sc2c1C1"

Scores: "IC50": 4.01, "QED": 0.699, "Novelty": Yes

Iteration 46: "reason": "Cyclopropylmethyl (4.01 nM) was worse than ethyl (2.47 nM) and
 ↪ added MW. Key 83 now contributes +0.16 which is good. Going back to best scaffold. Key
 ↪ 48 hurts (-0.12). Key 94 hurts (-0.10). I'll try reducing the number of oxygens to
 ↪ reduce key 48 penalty. Using a thioamide instead of amide on the diazepanone might
 ↪ help.", "smiles": "Fc1cc(CNC)c2nc(NC(=O)C3CCCN(CC)C(=S)N3C)sc2c1C1"

Scores: "IC50": 23.16, "QED": 0.690, "Novelty": Yes

Iteration 47: "reason": "Thioamide (23.16 nM) was much worse and triggered structural
 ↪ alert. Key 137 absence hurt badly (-0.30). Going back to best scaffold (2.47 nM). I'll
 ↪ try a minor modification - using N-methyl instead of N-ethyl on the diazepanone to
 ↪ reduce MW while keeping the methylaminomethyl group on benzothiazole.", "smiles":
 ↪ "Fc1cc(CNC)c2nc(NC(=O)C3CCCN(C)C(=O)N3C)sc2c1C1"

Scores: "IC50": 15.06, "QED": 0.807, "Novelty": Yes

Iteration 48: "reason": "N-methyl (15.06 nM) was worse than N-ethyl (2.47 nM). Key 115
 ↪ (CH3~*~CH2~*) and key 129 (CH2~*~*~CH2) are important. Going back to N-ethyl. Key 129
 ↪ absence hurts (-0.20). I'll try adding a propyl chain on the benzothiazole amine to
 ↪ create the CH2~*~*~CH2 pattern while keeping the successful diazepanone core.",
 ↪ "smiles": "Fc1cc(CNCCC)c2nc(NC(=O)C3CCCN(CC)C(=O)N3C)sc2c1C1"

Scores: "IC50": 3.22, "QED": 0.617, "Novelty": Yes

Iteration 49: "reason": "Propyl chain (3.22 nM) triggered structural alert for 4
 ↪ consecutive non-ring atoms. Going back to best scaffold (2.47 nM) with
 ↪ methylaminomethyl. Key 48 hurts (-0.11). I'll try replacing one carbonyl with a
 ↪ methylene to reduce key 48 penalty while keeping the 7-membered ring structure. Using
 ↪ a caprolactam-like ring instead of diazepanone.", "smiles":
 ↪ "Fc1cc(CNC)c2nc(NC(=O)C3CCCN(CC)CC3)sc2c1C1"

Scores: "IC50": 58.96, "QED": 0.802, "Novelty": Yes

Iteration 50: "reason": "Removing the lactam carbonyl (58.96 nM) was much worse - key 137
 ↪ absence hurt badly (-0.29). The diazepanone with two carbonyls is essential. Going
 ↪ back to best scaffold (2.47 nM). I'll try a small modification - adding a fluorine to
 ↪ the methylaminomethyl group to potentially improve binding without triggering
 ↪ alerts.",
 "smiles": "Fc1cc(C(F)NC)c2nc(NC(=O)C3CCCN(CC)C(=O)N3C)sc2c1C1"

Scores: "IC50": 5.52, "QED": 0.687, "Novelty": Yes

Finalisation:

Molecular Optimization Summary: Protease Inhibitor Development

Objective

Optimize a ligand for protease inhibition with IC50 < 1.00 nM, QED >= 0.60, and structural
↳ novelty (not in PubChem).

Optimization Trajectory

Initial Phase (Iterations 1-10): The campaign began with a peptidomimetic scaffold
↳ (IC50 = 94,377 nM) that showed poor activity. Early exploration identified
↳ sulfonamide-containing compounds with improved potency (~810 nM), though some lacked
↳ novelty. A benzothiazole scaffold emerged as promising (491 nM, iteration 4).

Scaffold Refinement (Iterations 11-20): Systematic optimization of the benzothiazole
↳ core revealed key structure-activity relationships. A fluorinated benzothiazole with
↳ cyclohexyl amide achieved 752 nM. Introduction of a piperidinone ring dramatically
↳ improved potency to 321 nM (iteration 16), and N-methylation of the lactam further
↳ enhanced activity to 169 nM (iteration 17).

Halogen Optimization (Iterations 21-28): Replacing fluorine with chlorine on the
↳ benzothiazole improved IC50 to 157 nM. A critical breakthrough came with dual
↳ halogenation (F and Cl adjacent), achieving 61.5 nM (iteration 28). N-ethyl
↳ substitution on the lactam proved superior to N-methyl, reaching 17.8 nM (iteration
↳ 29).

Final Optimization (Iterations 31-50): Addition of a methylaminomethyl group on the
↳ benzothiazole improved potency to 13.7 nM, then 9.4 nM with secondary amine
↳ optimization. Converting the piperidinone to a piperazinone achieved 7.5 nM. The
↳ breakthrough came with a 7-membered diazepanone ring system, reaching 2.47 nM
↳ (iteration 38) - the best result obtained.

Key Structural Features of Optimized Lead

- Core: 6-fluoro-7-chloro-benzothiazole with methylaminomethyl substituent
- Warhead: N-methyl-N'-ethyl-diazepan-2,5-dione linked via amide
- SMILES: `Fclcc(CNC)c2nc(NC(=O)C3CCCN(CC)C(=O)N3C)sc2c1Cl`
- IC50: 2.47 nM | QED: 0.767 | Novel: Yes

Critical SAR Insights

1. Dual halogens (F/Cl) on benzothiazole essential for potency
2. N-ethyl > N-methyl > N-propyl on lactam nitrogen
3. 7-membered diazepanone superior to 6-membered piperidinone
4. Methylaminomethyl substituent provides optimal balance of potency and drug-likeness

Conclusion

The optimization achieved a 38,000-fold improvement in potency from the initial compound,
↳ approaching but not reaching the 1.00 nM target. The final compound (2.47 nM)
↳ represents a novel, drug-like protease inhibitor candidate.